Mechanistic modelling of in vitro fermentation and methane production by rumen microbiota

Rafael Munoz Tamayo, Sylvie Giger-Reverdin, Daniel Sauvant

Mechanistic modelling of *in vitro* fermentation and methane production by rumen microbiota

Rafael Muñoz-Tamayo[a], Sylvie Giger-Reverdin[a], Daniel Sauvant[a]

[a] *UMR Modélisation Systémique Appliquée aux Ruminants, INRA, AgroParisTech, Université Paris-Saclay, 75005, Paris, France*

Abstract

Existing mechanistic models of the rumen ecosystem have proven to be useful to better understand and represent rumen fermentation. Opportunities for improving rumen fermentation models include a better representation of the microbiota, hydrogen dynamics and a mechanistic description of pH. The objective of this work was to include such aspects in the development of a mathematical model of rumen fermentation under *in vitro* conditions. The developed model integrates microbial metabolism, acid base reactions and liquid-gas transfer. Model construction was based on an aggregated representation of the hydrolysis of carbohydrates and proteins, and the further fermentation of soluble monomers. The model is a differential algebraic equation model with 18 compartments. One of the main contributions of the model developed here resides in the mechanistic description of pH, the use of biochemical reactions and partition rules to define the stoichiometry of fermentation, the representation of hydrogen metabolism, and the representation of the rumen microbiota into functional groups associated with the utilization of hexoses, amino acids and hydrogen. The model was calibrated with published data from a 2×2 factorial experiment devoted to assessing the relative importance of the type of inoculum and substrate on the fermentation pattern. The treatments were the level of concentrate in the substrate (low concentrate vs. high concentrate), and the inocula type (obtained from goats fed at low or high concentrate). The model was implemented in Matlab. The code is available on request for academic purposes. Model evaluation was performed by regression analysis and the calculation of statistical indicators using the model predicted values and observed values. The model was capable to represent in a satisfactory fashion the dynamics of the fermentation, that is the pH, the individual

Email address: rafael.munoztamayo@agropartistech.fr (Rafael Muñoz-Tamayo)

volatile fatty acids and the gas compounds, namely methane, hydrogen and carbon dioxide. The model predictions exhibited high concordance correlation coefficients (CCC) . For the pH and the CH_4, the CCC was of 0.91 and 0.93 respectively. For the other variables CCC>0.96. The model developed was instrumental to quantify the differences of the fermentation pattern between the treatment combinations. These differences were mainly captured by parameters related to the flux distribution and were found to be dependent mainly on the type of inoculum. For instance, the flux towards butyrate production from sugars utilization for the microbiota of the inoculum adapted to high concentrate was about 30% higher than that for the inoculum adapted to low concentrate. This result, however, requires further validation with new data. Further developments are needed to incorporate physiological *in vivo* factors into our model. Nevertheless, the structure developed here appears to be a promising approach for enhancing the mechanistic description of the rumen microbial ecosystem.

Keywords: anaerobic digestion; hydrogen; methane; pH; stoichiometry; volatile fatty acids

1. Introduction

The design of optimal nutritional strategies for ruminants with the target of maximizing animal performance and efficiency while reducing enteric methane emissions necessitates a thorough understanding of rumen fermentation. Mathematical models of rumen fermentation can be effective tools to contribute to the development of these feeding strategies. Naturally, to exploit such usefulness, the models must be able to represent the real system with an adequate degree of reliability. Mechanistic modelling provides a rational way of integrating knowledge and exploiting information for predicting system function. The development of mechanistic models of rumen fermentation has been a longstanding research activity in animal nutrition (*e.g.,* Baldwin et al. (1987); Dijkstra et al. (1992); Lescoat and Sauvant (1995); Bannink et al. (2006); Serment and Sauvant (2011); Mills et al. (2014)). However, the assessment of the limitations of current mechanistic models suggests that there is still room for model improvement to better predict the dynamical pattern of rumen fermentation, including H_2, CH_4 and VFA production (Offner and

Sauvant, 2004; Ellis et al., 2008; Alemu et al., 2011; Bannink et al., 2011; Vetharaniam et al., 2015). Some of the features to be tackled for improving the predictive capabilities of current mechanistic models include a better representation of the rumen microbiota and of hydrogen dynamics. The concentration of hydrogen in the rumen affects the pattern of fermentation (Janssen, 2010). Hydrogen utilization by microbes is central to maintaining an hydrogen level that allows the thermodynamic feasibility of the fermentation pathways (Offner and Sauvant, 2006; Janssen, 2010). Moreover, hydrogen is the main substrate for methane production. Additionally, progress on predicting ruminal pH is required since it is a central indicator of rumen status and function (Kohn and Boston, 2000; Dijkstra et al., 2012). Few works have actually addressed the mechanistic modelling of ruminal pH. In this respect, following the work of Kohn and Dunlap (1998), Imamidoost and Cant (2005) developed a model based on acid-base reactions, which provided satisfactory pH predictions. However, the model of Imamidoost and Cant (2005) underpredicted the concentration of organic acids. A similar approach was used by Serment and Sauvant (2011) to describe the pH under *in vitro* conditions. The model of Serment and Sauvant (2011) could predict with accuracy the pH dynamics only during the first hours of the fermentation. Another attempt at pH modelling within a thermodynamical framework of the rumen was presented by Offner and Sauvant (2006) but the accuracy of the predictions was unsatisfactory.

In this context, the objective of our work was to develop a mathematical model that contributes to a better mechanistic representation of rumen fermentation by closely coupling biological and physicochemical phenomena. The mathematical model herein developed extends the mechanistic model developed by Serment and Sauvant (2011), which was calibrated with experimental data resulting from an *in vitro* fermentation study of pea flour (Maaroufi et al., 2009) and assessed against *in vitro* experimental data from a wide range of feeds (Giger-Reverdin et al., 2014). The model developed by Serment and Sauvant (2011) was adequate in capturing the dynamical pattern of ammonia and gas production across a large variety of substrates. In contrast, model predictions of total VFA were less accurate and finally predictions of pH were rather unsatisfactory. The extensions that we pursued in the present work results in an alternative model structure compared to exist-

ing models of rumen fermentation. Our model development has the following features: *i*) it proposes an alternative representation of the rumen microbiota by the incorporation of three theoretical microbial functional groups responsible for the utilization of hexoses, amino acids and hydrogen, *ii*) it includes a mechanistic description of the pH by incorporating acid-base reactions, *iii*) it includes liquid-gas transfer phenomena for hydrogen, methane and carbon dioxide, and *iv*) it separates sugars and amino acids metabolism and the partition rules are defined by using knowledge on the main biochemical reactions of the fermentation.

2. Material and methods

2.1. Experimental case study

The model here developed was built on the basis of an *in vitro* experimental study devoted to quantify the effect and interaction of both inocula and substrates on ruminal fermentation (Serment et al., 2016). Two substrates differing in the proportion of concentrate were evaluated: a low (L_s) concentrate substrate (350 g kg^{-1} dry matter (DM) concentrate) versus a high (H_s) concentrate substrate (700 g kg^{-1}). The substrate was composed of grass hay, dehydrated alfalfa and concentrate as described by Serment (2012). The ingredient and analytical composition of these diets is presented in Table 1. Ruminal contents from adult goats in mid-lactation were used as inoculum. Two types of inocula were evaluated. The first inoculum (L_i) was composed of rumen fluids from three goats adapted to the L_s diet. The second inoculum (H_i) was composed of rumen fluids from three goats adapted to the H_s diet. The *in vitro* experiment was therefore defined by a 2×2 factorial design where the factors were the inoculum type (with levels L_i vs. H_i) and the substrate type (with levels L_s vs. H_s). The resulting four treatment combinations were L_iL_s, L_iH_s, H_iL_s, H_iH_s.

The experimental technique used in the work of Serment et al. (2016) is an adaptation of the syringe gas test (Menke et al., 1979) developed by Maaroufi et al. (2009) that allows to measure the fermentation dynamics. The fermentation took place during 24 h at constant temperature of 39°C. It was monitored by measurements of pH, acetate, butyrate, propionate, branched-chain volatile fatty acids, valerate and NH_3 at $t = 0, 3, 6, 9, 12, 24$

hours. The production of gas and its composition (CH_4, H_2 and CO_2) were measured for the time intervals: 0-3h, 3-12h, 12-24h. Experimental data are means of eight replicates. These data were used for estimating the parameters of the model.

2.2. Model development

The mathematical model was built on the following assumptions:

i) Two pools of carbohydrates are considered, namely cell wall (structural) carbohydrates, expressed as neutral detergent fibre (NDF), and non-structural carbohydrates (NSC). Following previous models of rumen fermentation, this distinction is made to account for the observed differences in degradation rates of feed carbohydrates. In our model, NSC does not include monosaccharides since they are represented separately as described below.

ii) Hydrolysis is an extracellular process that depends only on the concentration of polymers, *i.e.* carbohydrates and proteins. It is known that hydrolysis processes are carried out by multiple steps and are mediated by the enzymatic action of the microbes. However, it has been proposed that first-order kinetics reflect accurately the cumulative effect of the various processes involved in the hydrolysis (Waldo et al., 1972; Batstone et al., 2002). At this stage of our model development, we adopted the same premise.

iii) Hydrolysis of carbohydrates releases hexose monomers that are collectively represented by a unique compartment of glucose.

iv) Hydrolysis of proteins releases amino acids that are collectively represented by an average pool of amino acids treated as a unique compartment. Formation and hydrolysis of peptides are aggregated into the process of protein hydrolysis. The molecular formula of the average amino acid ($C_5H_{9.8}O_{2.7}N_{1.5}$) was calculated using the mean values of amino acids composition of dehydrated alfalfa obtained from Feedipedia (`http://www.feedipedia.org/`). The nitrogen content of the average amino acid was of 13.4%. The molecular formula was corrected to set the nitrogen content to the standard value of 16% used in ruminant nutrition (see Appendix A).

v) The rumen microbiota is represented by three theoretical functional groups. A functional group is determined by the microbial utilization of a soluble substrate in the fermentation pathway. The substrates available for microbial utilization are sugars (represented by glucose), amino acids (average) and hydrogen. Therefore, three microbial groups are accounted for, namely: sugars utilizers (x_{su}), amino acids utilizers (x_{aa}) and hydrogen utilizers ($x_{\mathrm{H_2}}$). The approach of representing the microbiota by several functional groups was not applied in the model of (Serment and Sauvant, 2011). However, it has been used to model the fermentation in the human colon (Muñoz-Tamayo et al., 2009) and in anaerobic reactors (Batstone et al., 2002). It should be noted that this representation differs from the traditional way of representing the rumen microbiota as fibre degraders and starch degraders (Dijkstra et al., 1992).

vi) Ammonia is assumed to be the sole source of nitrogen for sugars utilizers. This assumption is a simplification of the biochemistry of the fermentation, since sugars utilizers are able to use both NH_3 and amino acids as nitrogen source of microbial protein (Wallace et al., 1997). Our assumption is however consistent with microbiological studies with both cellulolytic and noncellulolytic ruminal bacteria that have shown that under ruminal physiological conditions, NH_3 provides in average 80% of microbial N (Atasoglu et al., 2001). In our model, the positive effect of amino acid on microbial growth of sugars utilizers is thus represented by the supply of NH_3 from deamination.

vii) Soluble substrates are utilized towards product formation and microbial growth. Substrate utilization depends on the concentration of the respective substrate and the microbial functional group.

viii) Dead microbial cells are recycled as source of proteins and carbohydrates.

ix) Acetate, propionate and butyrate are assumed to be the only VFAs produced during fermentation.

x) Acid-base reactions are considered as instantaneous.

xi) Microbial maintenance was not explicitly represented in our model, although some works assume that decay rates (as the death cell rate in our model) can take into

account maintenance (Xu et al., 2011; Sari and Harmand, 2016). Thus, microbial maintenance requirements were assumed to be negligible.

The model integrates metabolic conversions, liquid-gas transfer and acid-base reactions. The model comprises 18 ordinary differential equations resulting from mass balance equations for a batch system and algebraic equations representing the acid-base reactions. The resulting model is therefore a differential algebraic equation (DAE) model. The notation used in the model and the list of abbreviations used is shown in Table 2. In the next sections, model equations are detailed. We adopted the formalism used in mathematical models developed to describe the anaerobic digestion in reactors for waste water treatment (Batstone et al., 2002) and fermentation in the human colon (Muñoz-Tamayo et al., 2010). We have borrowed modelling concepts from the model developed by Batstone et al. (2002) (the Anaerobic Digestion Model No.1 (ADM1)) to define our model by considering the specificities of rumen fermentation. For example, the ADM1 includes reactions of VFA oxidation and acetoclastic methanogenesis. These reactions were not included in our model given that they are not relevant for the rumen ecosystem.

2.2.1. Microbial metabolism and liquid-gas transfer

To keep a relative simple structure, our model aggregated the metabolic pathways of rumen fermentation into a limited number of macroscopic reactions, which have been documented in the literature for a long time (Wolin et al., 1997). A scheme representing the mass fluxes of the fermentation process is shown in Fig. 1. The utilization of substrates in the fermentation drives two reaction processes namely product formation and microbial growth. In addition to these biological reactions, mass transfer phenomena of H_2, CH_4 and CO_2 between the liquid and gas phases occur.

The model has 18 state variables (compartments in Fig. 1) that correspond to the concentrations of polymer components (z_i, g/L), soluble components (s_i, mol/L), microbial functional groups (x_i, mol/L) and to the amount of components in the gas phase ($n_{g,i}$, moles). Polymer components are cell wall carbohydrates (z_{ndf}), non-structural carbohydrates (z_{nsc}) and proteins (z_{pro}). Soluble components are sugars (s_{su}), amino acids (s_{aa}), hydrogen ($s_{\mathrm{H_2}}$), acetate (s_{ac}), butyrate (s_{bu}), propionate (s_{pr}), inorganic nitrogen (s_{IN})

and inorganic carbon (s_{IC}). The inorganic carbon concentration s_{IC} is the sum of the concentrations of soluble carbon dioxide ($s_{\mathrm{CO_2}}$) plus bicarbonate ions ($s_{\mathrm{HCO_3^-}}$). Similarly, the inorganic nitrogen concentration s_{IN} is the sum of the concentrations of ammonia ($s_{\mathrm{NH_3}}$) plus ammonium ions ($s_{\mathrm{NH_4^+}}$). For the sake of readability, these relationships are not depicted in Fig. 1 but are further explained after the definition of equations (12) and (13). Microbial functional groups are sugars utilizers (x_{su}), amino acids utilizers (x_{aa}) and hydrogen utilizers ($x_{\mathrm{H_2}}$). Moles in the gas phase correspond to hydrogen ($n_{\mathrm{g,H_2}}$), carbon dioxide ($n_{\mathrm{g,CO_2}}$) and methane ($n_{\mathrm{g,CH_4}}$).

The breakdown and fermentation of feedstuffs by the rumen microbiota was represented in the model through nine biological processes: hydrolysis of cell wall carbohydrates (ρ_{ndf} (g/(L·h)), hydrolysis of non-fibre carbohydrates (ρ_{nsc} (g/(L·h)), hydrolysis of proteins (ρ_{pro} (g/(L·h)), utilization of sugars (ρ_{su} (mol/(L·h)), utilization of amino acids (ρ_{aa} (mol/(L·h)), utilization of hydrogen ($\rho_{\mathrm{H_2}}$ (mol/(L·h)) and the death of the three microbial groups ($\rho_{x_{\mathrm{su}}}, \rho_{x_{\mathrm{aa}}}, \rho_{\mathrm{H_2}}$) expressed in mol/(L·h). The mass transfer phenomena of H_2, CH_4 and CO_2 between the liquid and gas phases are represented by the kinetic rates $\rho_{\mathrm{T,H_2}}, \rho_{\mathrm{T,CH_4}}, \rho_{\mathrm{T,CO_2}}$, and are given in mol/(L·h).

The microbial process associated with utilization or hydrolysis of the component j is represented by the kinetic rate ρ_j, which is given in g/(L·h) or mol/(L·h). Hydrolysis and microbial death were described by first-order kinetics. Substrate utilization was described by Monod (Michaelis-Menten) kinetics. The Monod equation is the most widely used expression to describe microbial growth rate. The kinetic rate of substrate utilization (ρ_j) by Monod kinetics is

$$\rho_j = k_{\mathrm{m},j} \frac{s_j}{K_{\mathrm{s},j} + s_j} x_j \tag{1}$$

Where s_j and x_j represent respectively the substrate and the microbial biomass concentrations. The kinetic expression is defined by two parameters namely the maximum specific utilization rate constant of substrate ($k_{\mathrm{m},j}$) and the Monod constant ($K_{\mathrm{s},j}$). The maximum specific utilization rate constant of substrate relates to microbial activity, and the Monod constant relates to substrate affinity of the microbes. These parameters will be defined in the parameter estimation strategy, as it will be explained later. To account for nitrogen limitation on the rates of sugars and hydrogen utilization, and additional

factor was included in the respective kinetic expressions (see Table 3). Monod kinetics is a comprehensive equation that has the advantage of being defined by parameters with biological meaning.

The formation or consumption of the component j in the process described by the kinetic rate ρ_j is defined via the yield factors as summarized in Table 3. This way of representation, sometimes denoted as the Petersen matrix (Petersen, 1965), is well suited for displaying the stoichiometry of the fermentation through the yield factors ($Y_j, Y_{i,j}$). This type of approach has been already applied at the elementary level of rumen fermentation (Reichl and Baldwin, 1975) and allows to reducing substantially the number of model parameters to be estimated. Referring to the Table 3, one mole of substrate s_j utilized produces Y_j moles of microbial biomass. The amount of moles of the compound s_i that is either produced or consumed during the substrate utilization of s_j is given by the yield factor $Y_{i,j}$. The link between yield factors and stoichiometry will be explained in the next section.

On the basis of the previous statements on model structure, we proceed to detail the equations of the model. By applying mass balances, we obtain the following equations.

For polymer components

$$\frac{\mathrm{d}z_{\mathrm{ndf}}}{\mathrm{d}t} = -\rho_{\mathrm{ndf}} \tag{2}$$

$$\frac{\mathrm{d}z_{\mathrm{nsc}}}{\mathrm{d}t} = -\rho_{\mathrm{nsc}} + (f_{\mathrm{ch,x}} \cdot w_{\mathrm{mb}}) \cdot \left(\rho_{x_{\mathrm{su}}} + \rho_{x_{\mathrm{aa}}} + \rho_{x_{\mathrm{H_2}}}\right) \tag{3}$$

$$\frac{\mathrm{d}z_{\mathrm{pro}}}{\mathrm{d}t} = -\rho_{\mathrm{pro}} + (f_{\mathrm{pro,x}} \cdot w_{\mathrm{mb}}) \cdot \left(\rho_{x_{\mathrm{su}}} + \rho_{x_{\mathrm{aa}}} + \rho_{x_{\mathrm{H_2}}}\right) \tag{4}$$

Where $\rho_{\mathrm{ndf}}, \rho_{\mathrm{nsc}}, \rho_{\mathrm{pro}}$ are the hydrolysis rates of the polymers, described by first-order kinetics with respect to the substrate (g/(L·h)). The second terms in the right-hand side of equations (3) and (4) represent the recycling of dead microbial cells. The rate of dead of microbial cells is determined by the parameter k_{d} (1/h) (Table 3). The parameters $f_{\mathrm{ch,x}}, f_{\mathrm{pro,x}}$ are the fractions of carbohydrates and proteins by weight of microbial cells. The molecular weight of microbial cells is w_{mb} (Table 2).

For soluble components

$$\frac{\mathrm{d}s_{\mathrm{su}}}{\mathrm{d}t} = \rho_{\mathrm{ndf}}/w_{\mathrm{su}} + \rho_{\mathrm{nsc}}/w_{\mathrm{su}} - \rho_{\mathrm{su}} \tag{5}$$

$$\frac{\mathrm{d}s_{\mathrm{aa}}}{\mathrm{d}t} = \rho_{\mathrm{pro}}/w_{\mathrm{aa}} - \rho_{\mathrm{aa}} \tag{6}$$

$$\frac{\mathrm{d}s_{\mathrm{H_2}}}{\mathrm{d}t} = Y_{\mathrm{H_2,aa}} \cdot \rho_{\mathrm{aa}} + Y_{\mathrm{H_2,su}} \cdot \rho_{\mathrm{su}} - \rho_{\mathrm{H_2}} - \rho_{\mathrm{T,H_2}} \tag{7}$$

$$\frac{\mathrm{d}s_{\mathrm{ac}}}{\mathrm{d}t} = Y_{\mathrm{ac,su}} \cdot \rho_{\mathrm{su}} + Y_{\mathrm{ac,aa}} \cdot \rho_{\mathrm{aa}} \tag{8}$$

$$\frac{\mathrm{d}s_{\mathrm{bu}}}{\mathrm{d}t} = Y_{\mathrm{bu,su}} \cdot \rho_{\mathrm{su}} + Y_{\mathrm{bu,aa}} \cdot \rho_{\mathrm{aa}} \tag{9}$$

$$\frac{\mathrm{d}s_{\mathrm{pr}}}{\mathrm{d}t} = Y_{\mathrm{pr,su}} \cdot \rho_{\mathrm{su}} + Y_{\mathrm{pr,aa}} \cdot \rho_{\mathrm{aa}} \tag{10}$$

$$\frac{\mathrm{d}s_{\mathrm{CH_4}}}{\mathrm{d}t} = Y_{\mathrm{CH4,H_2}} \cdot \rho_{\mathrm{H_2}} - \rho_{\mathrm{T,CH_4}} \tag{11}$$

To illustrate the structure of the model, let us consider the dynamics of sugars concentration (s_{su}), which has a molecular weight of w_{su}. Sugars are produced from the hydrolysis of cell wall carbohydrates (z_{ndf}) and non-structural carbohydrates (z_{nsc}). The hydrolysis rates are represented by ρ_{ndf} and ρ_{nsc} respectively. Sugars are further fermented (following the kinetic rate ρ_{su}) and produces, among other metabolites, acetate and H_2 with a stoichiometry given by the yield factors $Y_{\mathrm{ac,su}}$ and $Y_{\mathrm{H_2,su}}$ respectively. Hydrogen in the liquid phase is utilized by the microbes following the kinetic rate $\rho_{\mathrm{H_2}}$ and participates in a mass transfer phenomena with the hydrogen pool of the gas phase. This transfer is represented by the kinetic rate $\rho_{\mathrm{T,H_2}}$.

The concentrations of individual VFAs are the sum of the concentrations of the ionic (conjugate base) and free (undisocciated) forms. So, instead of modelling the individual acid and base forms, we model the total VFA and one of the acid-base components. This choice was made to facilitate the implementation of the model (Rosen et al., 2006). This same reasoning was applied for the couples $s_{\mathrm{CO_2}} \leftrightarrow s_{\mathrm{HCO_3^-}}$ (gathered in the variable s_{IC}) and $s_{\mathrm{NH_3}} \leftrightarrow s_{\mathrm{NH_4^+}}$ (gathered in the variable s_{IN}). The dynamics of s_{IC} and s_{IN} are defined as follows.

$$\frac{\mathrm{d}s_{\mathrm{IC}}}{\mathrm{d}t} = Y_{\mathrm{IC,aa}} \cdot \rho_{\mathrm{aa}} + Y_{\mathrm{IC,su}} \cdot \rho_{\mathrm{su}} + Y_{\mathrm{IC,H_2}} \cdot \rho_{\mathrm{H_2}} - \rho_{\mathrm{T,CO_2}} \tag{12}$$

$$\frac{\mathrm{d}s_{\mathrm{IN}}}{\mathrm{d}t} = Y_{\mathrm{IN,aa}} \cdot \rho_{\mathrm{aa}} + Y_{\mathrm{IN,su}} \cdot \rho_{\mathrm{su}} + Y_{\mathrm{IN,H_2}} \cdot \rho_{\mathrm{H_2}} \tag{13}$$

For microbial functional groups

$$\frac{\mathrm{d}x_{\mathrm{su}}}{\mathrm{d}t} = Y_{\mathrm{su}} \cdot \rho_{\mathrm{su}} - \rho_{x_{\mathrm{su}}} \tag{14}$$

$$\frac{\mathrm{d}x_{\mathrm{aa}}}{\mathrm{d}t} = Y_{\mathrm{aa}} \cdot \rho_{\mathrm{aa}} - \rho_{x_{\mathrm{aa}}} \tag{15}$$

$$\frac{\mathrm{d}x_{\mathrm{H_2}}}{\mathrm{d}t} = Y_{\mathrm{H_2}} \cdot \rho_{\mathrm{H_2}} - \rho_{x_{\mathrm{H_2}}} \tag{16}$$

It should be noted that the fermentation reactions have been defined on the basis of the kinetic rate of substrate utilization (ρ_j). In some works, the growth rate (μ_j) is rather used. If maintenance requirements are negligible as presently stated, the growth and substrate utilization rates are related by

$$\mu_j = Y_j \cdot \rho_j \tag{17}$$

The maximal growth rate occurs when the substrate utilization is maximal. It is important to note that in the model structure used here, the microbial yields Y_j are actually linked to the ATP derived from the reactions of product formation as it will be explained in the next section.

Now, for the gas phase, we have

$$\frac{\mathrm{d}n_{\mathrm{g,H_2}}}{\mathrm{d}t} = V_l \cdot \rho_{\mathrm{T,H_2}} \tag{18}$$

$$\frac{\mathrm{d}n_{\mathrm{g,CO_2}}}{\mathrm{d}t} = V_l \cdot \rho_{\mathrm{T,CO_2}} \tag{19}$$

$$\frac{\mathrm{d}n_{\mathrm{g,CH_4}}}{\mathrm{d}t} = V_l \cdot \rho_{\mathrm{T,CH_4}} \tag{20}$$

The term $\rho_{\mathrm{T,i}}$ represents the liquid-gas transfer rate (at non-equilibria), described as

$$\rho_{\mathrm{T,H_2}} = k_{\mathrm{L}}\mathrm{a} \cdot \left(s_{\mathrm{H_2}} - K_{\mathrm{H,H_2}} \cdot p_{\mathrm{g,H_2}}\right) \tag{21}$$

$$\rho_{\mathrm{T,CO_2}} = k_{\mathrm{L}}\mathrm{a} \cdot \left(s_{\mathrm{CO_2}} - K_{\mathrm{H,CO_2}} \cdot p_{\mathrm{g,CO_2}}\right) \tag{22}$$

$$\rho_{\mathrm{T,CH_4}} = k_{\mathrm{L}}\mathrm{a} \cdot \left(s_{\mathrm{CH_4}} - K_{\mathrm{H,CH_4}} \cdot p_{\mathrm{g,CH_4}}\right) \tag{23}$$

Where $k_{\mathrm{L}}\mathrm{a}$ (h^{-1}) is the mass transfer coefficient, $K_{\mathrm{H},i}$ (M/bar) is the Henry's law coefficient and $p_{\mathrm{g},i}$ (bars) is the partial pressure of component i. For simplification, we assumed that the total pressure in the gas phase was constant. Its value was set to $P = 1.01325$ bars. Therefore, the partial pressure of component i satisfies

$$p_{\mathrm{g},i} = \frac{n_{\mathrm{g},i}}{\sum_{i=1}^{3} n_{\mathrm{g},i}} P \tag{24}$$

2.2.2. Stoichiometry of the fermentation

The yield factors defined in the model can be estimated experimentally or via parameter estimation. In our case, we have capitalized on the knowledge of the stoichiometry of certain well known reactions to favour a mechanistic representation of metabolism and to reducing the dimension of unknown parameters. For the microbial utilization of sugars (glucose) and hydrogen, the reactions accounted for by the model are given in Table 4. The microbial fermentation profile is defined by the partitioning of fluxes between product formation and microbial growth reactions. To define the stoichiometry of the microbial growth reaction, it was assumed that the microbes have an average molecular formula of $C_5H_7O_2N$ (Batstone et al., 2002).

To illustrate how the yield factors were calculated, let us consider the utilization of sugars described in the model by reactions R_1-R_4 in Table 4. Firstly, it should be noted that reaction R_2 associated with propionate formation also produces acetate. Some works on rumen stoichiometry consider as possible pathway for propionate formation the reaction:

$$C_6H_{12}O_6 + 2H_2 \Rightarrow 2CH_3CH_2COOH + 2H_2O$$

However, propionate production by rumen microbes concomitantly occurs with acetate production as identified in the fermentation pathway of the predominant propionate producer *Selenomonas ruminantium* (Wolin et al., 1997). For these reasons, we decided to use the reaction R_2 (Table 4) as the main pathway of propionate formation.

As previously mentioned, substrate conversion is directed to reactions of product formation and microbial growth. The balance of these two processes is coupled to the cofactor ATP/ADP. In our model, the partition of substrate is parameterized as follows. The fraction of glucose utilized for microbial growth is defined by the microbial yield factor Y_{su} (which is linked to the ATP available from microbial synthesis). Let f_{su} be the fraction of sugars that is utilized for product formation. From the reaction R_4 of the Table 4, it follows that

$$f_{\mathrm{su}} = 1 - \frac{5}{6} Y_{\mathrm{su}} \tag{25}$$

Now, the utilization of sugars for product formation occurs only via the reactions R_1-R_3. Let λ_k denote the fraction of the sugars utilized via reaction k of Table 4, such that $\sum_{k=1}^{3} \lambda_k = 1$ to respect mass conservation. The yield factors for sugars utilization can thus be defined as follows

$$Y_{\mathrm{ac,su}} = f_{\mathrm{su}} \cdot (2 \cdot \lambda_1 + 2/3 \cdot \lambda_2) \tag{26}$$

$$Y_{\mathrm{bu,su}} = f_{\mathrm{su}} \cdot (\lambda_3) \tag{27}$$

$$Y_{\mathrm{pr,su}} = f_{\mathrm{su}} \cdot (4/3 \cdot \lambda_2) \tag{28}$$

$$Y_{\mathrm{H_2,su}} = f_{\mathrm{su}} \cdot (4 \cdot \lambda_1 + 2 \cdot \lambda_3) \tag{29}$$

$$Y_{\mathrm{IN,su}} = -Y_{\mathrm{su}} \tag{30}$$

$$Y_{\mathrm{IC,su}} = f_{\mathrm{su}} \cdot (2 \cdot \lambda_1 + 2/3 \cdot \lambda_2 + 2 \cdot \lambda_3) \tag{31}$$

Note that by using the stoichiometry of the reactions, we only need three parameters to be estimated ($Y_{\mathrm{su}}, \lambda_1, \lambda_2$) to define all the yield factors for sugars utilization. Without including the stoichiometry, we would have to estimate seven parameters.

Applying the same principles for hydrogen utilization, we obtain the following relationships for determining the yield factors.

$$f_{\mathrm{H_2}} = 1 - 10 Y_{\mathrm{H_2}} \tag{32}$$

$$Y_{\mathrm{CH_4,H_2}} = f_{\mathrm{H_2}} \cdot (1/4) \tag{33}$$

$$Y_{\mathrm{IC,H_2}} = -\left((1/4) \cdot f_{\mathrm{H_2}} + (5/10) \cdot (1 - f_{\mathrm{H_2}})\right) \tag{34}$$

$$Y_{\mathrm{IN,H_2}} = -Y_{\mathrm{H_2}} \tag{35}$$

For amino acids utilization, on the basis of amino acid composition from alfalfa, a theoretical reaction of the overall fermentation was derived (R5 in Table 4). This overall reaction was obtained by selecting the main fermentation reactions of individual amino acids for anaerobic bacteria. Following the procedure proposed by Ramsay and Pullammanappallil (2001), the overall reaction results from weighing the individual reactions by the molar composition of the feed. The procedure for deriving the overall fermentation reaction is detailed in Appendix A. The yield factor of component i ($Y_{i,\mathrm{aa}}$) is defined by the following equation

$$Y_{i,\mathrm{aa}} = (1 - Y_{\mathrm{aa}}) \cdot \sigma_{i,\mathrm{aa}} \tag{36}$$

Where the parameter $\sigma_{i,\mathrm{aa}}$ is the stoichiometric coefficient of the overall product formation reaction.

To respect the elementary balance of nitrogen, we set the following relationship:

$$Y_{\mathrm{IN,aa}} = N_{\mathrm{aa}} - Y_{\mathrm{aa}} \cdot N_{\mathrm{mb}} \tag{37}$$

with Y_{aa} (mol/mol) and $Y_{\mathrm{IN,aa}}$ (mol/mol) the yield factors of microbial cells and inorganic nitrogen during amino acids utilization. N_{mb} is the molar fraction of nitrogen of the microbial cells, N_{aa} the nitrogen molar fraction of the average amino acid.

It should be stressed that using biochemical reactions to defining the stoichiometry allows the automatic maintaining of elementary balances and reduces the number of unknown parameters of the model.

2.2.3. Acid-base reactions, charge balance and pH

Bases and acid compounds are made up by acid-base pairs. It follows that

$$s_{\mathrm{IC}} = s_{\mathrm{HCO_3^-}} + s_{\mathrm{CO_2}} \tag{38}$$

$$s_{\mathrm{IN}} = s_{\mathrm{NH_4^+}} + s_{\mathrm{NH_3}} \tag{39}$$

$$s_{\mathrm{ac}} = s_{\mathrm{ac^-}} + s_{\mathrm{hac}} \tag{40}$$

$$s_{\mathrm{bu}} = s_{\mathrm{bu^-}} + s_{\mathrm{hbu}} \tag{41}$$

$$s_{\mathrm{pr}} = s_{\mathrm{pr^-}} + s_{\mathrm{hpr}} \tag{42}$$

For the VFAs, for instance acetate, $s_{\mathrm{ac^-}}$ and s_{hac} are the concentrations of the VFA in ionic and free forms respectively.

By using the acid-base equilibrium equations, the concentrations of the ions are for-

mulated as functions of the concentration of the hydrogen ion s_{H^+}

$$s_{HCO_3^-} = \frac{K_{a,CO_2} s_{IC}}{K_{a,CO_2} + s_{H^+}} \tag{43}$$

$$s_{NH_4^+} = \frac{s_{IN} s_{H^+}}{K_{a,NH_4} + s_{H^+}} \tag{44}$$

$$s_{ac^-} = \frac{K_{a,ac} s_{ac}}{K_{a,ac} + s_{H^+}} \tag{45}$$

$$s_{bu^-} = \frac{K_{a,bu} s_{bu}}{K_{a,bu} + s_{H^+}} \tag{46}$$

$$s_{pr^-} = \frac{K_{a,pr} s_{pr}}{K_{a,pr} + s_{H^+}} \tag{47}$$

$$s_{OH^-} = \frac{K_w}{s_{H^+}} \tag{48}$$

Since the equilibrium constants (and pKa values) for the VFA are very close (see,*e.g.*, Kohn and Dunlap (1998)), we decided to simplify by aggregating the three acid-base reactions of VFA into a single one, that is

$$s_{VFA^-} = \frac{K_{a,VFA} s_{VFA}}{K_{a,VFA} + s_{H^+}} \tag{49}$$

With $s_{VFA^-} = s_{ac^-} + s_{bu^-} + s_{pr^-}$ and $s_{VFA} = s_{ac} + s_{bu} + s_{pr}$. This approach favours the mathematical treatment of the equations and does not have significant implications on the model output.

The pH of the medium is determined by the charge balance between the cations and anions from the acid-base reactions. It follows that the sum of cations minus the sum of anions must be equal to zero. Therefore

$$s_{cat^+} + s_{NH_4^+} + s_{H^+} - \left(s_{HCO_3^-} + s_{VFA^-} + s_{OH^-}\right) = 0 \tag{50}$$

In Equation (50), s_{cat^+} represents the balance of cations and anions of the medium that are not modelled. They referred to metallic ions. For the medium solution, we only considered bicarbonate in the model. However, the medium is actually composed of buffer and mineral solutions that contains components such phosphate (Menke et al., 1979) that have an effect on the pH. Using experimental data at t=0, we calculated the concentration of $s_{HCO_3^-}$ needed to make the charge balance equal to zero. Without including s_{cat^+}, the bicarbonate concentration was negative, which has no physical meaning. Thus, it was

essential to include the metallic ions s_{cat^+}. We assumed that s_{cat^+} remains constant over the fermentation.

By inserting equations (43),(44),(48) and (49) into equation (50), we obtain a polynomial of degree five with s_{H^+} as independent variable. The structure of the polynomial makes that it has a unique real positive root. At each time step, the polynomial is solved to find s_{H^+}. The pH is therefore determined by $\text{pH} = -log_{10}[s_{\text{H}^+}]$.

The model was implemented in Matlab® following guidelines for models of anaerobic digestion in reactors for waste water treatment (Batstone et al., 2002; Rosen et al., 2006). The Matlab code is available on request for academic purposes. The resulting model presents multiple time scales. For instance, while hydrolysis processes are characterized by time constants that can be of the order of days, acid-base equilibrium reactions take place almost instantaneously. In numerical computation, this property is also referred to as stiffness. Model simulation was carried out with the Matlab ODE solver ode23s. The algorithm used in ode23s is based on a modified Rosenbrock formula of order 2, adapted to stiff models (Shampine and Reichelt, 1997).

2.3. Parameter estimation and statistical analysis

For the parameter estimation routine, we aimed at reducing the number of parameters to be estimated. Accordingly, some parameters were set to be known and common to all the treatment combinations. The values of these parameters were extracted from the literature. Most of the physicochemical parameters were fixed to known values reported by Batstone et al. (2002) and extracted from the operational conditions of the experimental study of Serment et al. (2016). The values reported by Batstone et al. (2002) for the CO_2 and bicarbonate system are very similar to values reported for the rumen (Hille et al., 2016). Only k_{L}a and s_{cat^+} were estimated.

The biological parameters that were fixed were the hydrolysis rate constant of cell wall carbohydrates, the death cell rate constant (assumed to be the same for all microbes in all experimental conditions), the fraction of carbohydrates and protein of the microbial biomasses, the stoichiometric coefficients for amino acid fermentation, the nitrogen limitation constant, and the affinity Monod constants for the utilization of sugars, amino acids

and hydrogen. The hydrolysis rate constant for cell wall carbohydrates was set constant because different studies have shown that digestibility of NDF appears to be unaffected by the level of concentrate (Nagadi et al., 2000; Serment et al., 2011). Setting the values of the affinity constants reduces the difficulties associated with practical identifiability problems (*e.g.* high correlation between the parameters of Monod kinetics). Table 5 shows the primary sources used to extract the parameter values. Estimation was therefore performed for the hydrolysis rate constants of non-structural carbohydrates and protein, the maximum specific utilization rate constants of substrates, the microbial yield factors and the parameters related to the flux distribution for sugars and amino acid utilization. The parameter estimation was performed independently for each treatment combination. At $t0$, on the basis of microbiological data (Krause and Russell, 1996; Morgavi et al., 2010), the composition of the microbiota was set as 94% of sugar utilizers, 5 % of amino acids utilizers and 1 % of methanogens. The initial guess for the total microbial concentration was extracted from reported values of *in vitro* rumen fermentation (Nagadi et al., 2000). In the study of Serment et al. (2016), the incubation of blanks (inoculum without addition of substrate) showed that the inoculum was biologically active and that it contained enough energy sources to allow the fermentation to proceed towards VFA and methane production. Therefore, the parameter estimation was set to consider the contribution of NSC and protein of the inoculum. The initial concentration of sugars were set to 0.67 mM which is the range reported for the rumen (Janssen, 2010). Initial conditions for dissolved hydrogen and methane were taken from Wang et al. (2016a) and were set to 2 μM and 0.7 mM for hydrogen and methane respectively. Initial guess values used for the estimation were taken from studies of rumen and anaerobic microbial ecosystems (Robinson and Tiedje, 1982; Baldwin et al., 1987; Batstone et al., 2002).

Parameter estimation was performed with the Matlab® toolbox IDEAS (Muñoz-Tamayo et al., 2009), which is freely available at
`http://www.inra.fr/miaj/public/logiciels/ideas/index.html`.
We used the maximum likelihood estimator that minimizes

$$J(\boldsymbol{\theta}) = \sum_{k=1}^{n_{\mathrm{y}}} \frac{n_{\mathrm{t},k}}{2} \ln \left[\sum_{\mathrm{i}=1}^{n_{\mathrm{t},k}} [y_k(t_{i_k}) - y_{\mathrm{m}_k}(t_{i_k}, \boldsymbol{\theta})]^2 \right] \tag{51}$$

With n_{y} the number of measured (observed) variables and $n_{\mathrm{t},k}$ the number of observation times for the kth variable. The observed variables are

$\{s_{\mathrm{ac}}, s_{\mathrm{bu}}, s_{\mathrm{pr}}, s_{\mathrm{IN}}, n_{\mathrm{g,H_2}}, n_{\mathrm{g,CO_2}}, n_{\mathrm{g,CH_4}}, \mathrm{pH}\}$

Equation (51) applies to the case of asynchronous measurements (see Walter and Pronzato (1997)). This equation is adapted to our experimental case study. The Nelder-Mead Simplex method (Lagarias et al., 1998) was used as the optimization algorithm. Upper and lower bounds were imposed to force the parameters to lie on the interval of values reported in the literature.

The model was evaluated by regression analysis of observed values against predicted values as suggested by Piñeiro et al. (2008). The root mean squared error (RMSE) was calculated as a statistics of model performance. The agreement between observed values and predicted values was assessed by the concordance correlation coefficient (CCC) proposed by Lin (1989). Statistical analyzes were performed with Matlab®.

3. Results

3.1. Dynamical description of in vitro fermentation and model evaluation

Figures 2 and 3 display the *in vitro* data obtained from Serment et al. (2016) and the response of the calibrated model. A common scale is used to facilitate the comparison between the responses of the two inocula. The model satisfactorily captures the dynamics of all variables. It is worth noting that the model is able to represent the inflexions of the pH dynamics. This dynamic behaviour of the pH is also observed *in vivo* after feeding. Figure 4 summarizes the results by plotting the observations against model predictions. Table 6 summarizes the results of the regression analysis. For all variables, the intercept constants were not significant different from zero (p-value$>$ 0.05) and the slopes of the regression lines were not different from one (with the exception of the regression curves for propionate, CH_4 and CO2). The regression line for CO_2 had the slowest slope (0.86) while the regression line of CH_4 had the highest one (1.23). This means that the model predictions of the amount of CH_4 are about 81% of the experimental data and the amount of CO_2 are about 1.16% of the experimental data. We will need to challenge the model against a new set of data to identify if the underprediction of CH_4 and overprediction of

CO_2 are related to the experimental device analyzed or whether the model parameters require further refinement.

The pH exhibited the lowest determination coefficient ($r^2 = 0.83$) (Table 6), whereas for the other variables $r^2 \geq 0.97$. The model predictions exhibited high concordance correlation coefficients (CCC). For the pH and the CH_4, the CCC was of 0.91 and 0.93 respectively. For the other variables CCC$\geq$0.96. The pH had the lowest coefficient of variation of the RMSE (CV(RMSE)). The components in the gas phase had the higher CV(RMSE) (11%-25%), while the components in the liquid phase had in average a CV(RMSE) of 4.9%.

Figure 5 displays the predicted dynamics of the non measured variables for all the treatment combinations. The concentration of carbohydrate and protein polymers decreased in time as result of the hydrolysis. Sugars followed a monotonic decreasing dynamics, implying that the rate of sugars utilization was always faster than the rate of hexose release from carbohydrate hydrolysis. It is observed that the dynamics of carbohydrates, protein and sugars is very similar among the treatment combinations and the curve responses tend to overlap. For non-structural carbohydrates, it is observed that its initial concentration is higher for the experiments with the inoculum H_i than for the inoculum L_i.

For the average amino acid, it was observed that at the beginning of the fermentation, the production rate of amino acids from protein hydrolysis was higher than the amino acid utilization rate. After 2 h, microbes utilized amino acids at a higher rate than the protein hydrolysis rate. During the experimentation time all the microbial groups exhibited a growth rate higher than the decay rate. The dynamics of the microbial groups for the experiments with the same type of inoculum almost overlap. It is noted that the concentration of microbial biomass for the inoculum adapted to the high concentrate is higher than that of the inoculum adapted to the low concentrate, which is in agreement with the measurements reported by Nagadi et al. (2000). At the end of the fermentation, the microbiota was composed in average by 91.7% of sugars utilizers, 7.3% of amino acids utilizers and 1.0% of hydrogen utilizers.

Overall the predicted concentrations of sugars, amino acids, dissolved hydrogen and

methane are in agreement with values reported in the rumen literature (Atasoglu et al., 2001; Wang et al., 2016a; Janssen, 2010).

3.2. Model parameters

Table 5 shows the numerical values of parameters. The model has in total 9 physicochemical parameters and 23 biological parameters (operational parameters such as pressure (P) and temperature (T), and the molecular weights of compounds are not counted). Figure 6 displays the estimated parameters for each treatment combination. Only two physicochemical parameters ($k_{\mathrm{L}}\mathrm{a}$, s_{cat^+}) were estimated. Their estimated values did not exhibit significant differences among the treatments, which was expected. The liquid-gas transfer coefficient $k_{\mathrm{L}}\mathrm{a}$ is specific to the *in vitro* system utilized and s_{cat^+} is mainly determined by the buffer solution used in the medium, which has the same concentration for all experiments.

From the set of biological parameters, 13 parameters were set as known. In defining these biological parameters, we assumed a constant composition of biomass in terms of proteins and carbohydrates for all microbial groups. Additionally, we set the death cell rate to be the same for all microbes in all experimental conditions. We assumed that the substrate affinity for sugars, amino acids and hydrogen by the rumen microbiota are similar among the four treatment combinations. The affinity constants for sugars and amino acids were taken from (Baldwin et al., 1987). For hydrogen utilizers, the affinity constant was set as an average value reported for rumen microbes (Robinson and Tiedje, 1982). Stoichiometric coefficients for amino acid fermentation were derived from biochemical knowledge (see Appendix A).

Given the limited number of experiments analyzed in this work, it will be incautious to provide general statements about the validity of the estimated parameters to represent rumen fermentation in a broader context than the experimental study analyzed here. In spite of these limitations, the following analysis can be derived from the results. In Table 5, it is shown that the non-structural carbohydrates exhibited very similar hydrolysis rate constants among the experiments. The hydrolysis rate constants of NSC are higher than the hydrolysis rate constant of NDF (Table 5, which is biologically consis-

tent). Concerning protein hydrolysis, the hydrolysis rate constants are of the same order of magnitude than those for non-structural carbohydrates. The inoculum H_i adapted to the high concentrate diet appears to have a slightly higher hydrolysis rate constant of proteins than that of the inoculum L_i.

Concerning sugars utilization, the maximum specific utilization rate constant of sugars was the same for all experiments. The microbial yield for sugars utilization has an average value of 0.16 mol/mol. This value has the same order of magnitude of yield factors reported for utilization of glucose by rumen microbes (Russell and Wallace, 1997). There is not a clear dependency of the microbial yield factors with respect to either the inoculum or substrate.

Concerning amino acid utilization, the maximum specific utilization rate constant and the yield factors appear to be clustered with respect to the type of the inoculum. The group of amino acid utilizers of the inoculum L_i adapted to the low concentrate diet appears to have a higher growth than the microbial group of the inoculum H_i.

For hydrogen utilization, the microbial yield factors are the same for all the treatment combinations. The value corresponds to the lower bound used for constraining the optimization. This was done to allow the parameters to fall in a biological plausible space. The maximum specific utilization rate constant has an average value of 13.93 mol/(mol·h), which is in agreement with values reported for methanogens in reactors (Batstone et al., 2002).

From these results, we suggest that overall, the average values of the kinetic parameters ($k_{\mathrm{m,j}}, Y_j, Y_{i,j}$) can be used to represent the fermentation, with the exception of the parameters associated to amino acid utilization. However, since neither amino acids nor the microbial group related to their utilization were measured, new experiments are needed to confirm the specificity of amino acid utilization with respect to the substrate and inoculum. We suggest that the differences of the fermentation pattern between the treatment combinations are mainly due to the parameters associated to flux distribution (λ_1, λ_2), which seem to depend to the type of the inoculum (Fig. 6). For example, in the experiments with the inoculum H_i, the direction of fluxes towards butyrate production from sugars utilization (λ_3) is about 30% higher than that for the inoculum L_i (Table 5).

However, further validation with new data is required to confirm this hypothesis.

4. Discussion

The objective of this work was to develop a mathematical model of rumen *in vitro* fermentation by taking into consideration some aspects that have been identified as central for the improvement of rumen fermentation models. These aspects include a better representation of the microbiota, hydrogen dynamics and a mechanistic description of pH. The resulting model was effective in describing data of four *in vitro* treatment combinations, which indicates the strengthen of its structure to represent fermentation.

Initially, our strategy of model construction used mainly as conceptual basis the model developed by Serment and Sauvant (2011). The extensions that we pursued resulted in a mathematical model that partially differs to the model of Serment and Sauvant (2011). A major difference of our approach compared to the model of Serment and Sauvant (2011) is the representation of the microbiota as three functional groups associated with the specific utilization of sugars, amino acids and hydrogen. Other differences relate to the incorporation of macroscopic biochemical reactions to define the yield factors that determine the fermentation pattern, including the individual VFA. While Serment and Sauvant (2011) related methane production rate to the global fermentation rate of the soluble carbohydrates compartment, we incorporated a hydrogen compartment that enabled us to explicitly represent the methanogenesis reaction and define partition rules of hydrogen. This approach will be helpful to further developments for describing the determinants of hydrogen fluxes in the rumen. In relation to the pH, our model is based on the computation of the hydrogen ion concentration needed to balance the charges in the acid-base equilibrium reactions, while in the model of Serment and Sauvant (2011), the pH was determined by the equilibrium state of an acid-base reaction that aggregates the bicarbonate and the total VFAs. The improvement in fitting capabilities of our model suggests that the model developments performed here are useful.

In terms of model structure, we have borrowed modelling concepts from the Anaerobic Digestion Model No.1 (ADM1) (Batstone et al., 2002). The ADM1 was developed by international experts in the domain of anaerobic digestion processes for waste water treat-

ment. The ADM1 model is the result of a consensus of the state of the art in anaerobic digestion models, and it has been consolidated as a common modelling platform in the engineering community. The ADM1 has been used in a large number of applications and has also enriched the discussion between scholars for identifying key aspects for model improvement. Moreover, The ADM1 has been used as a basis for model developments of the fermentation in the human colon (Muñoz-Tamayo et al., 2010; Motelica-Wagenaar et al., 2014). The fermentation pathway as described in the original structure of ADM1 does not apply to the rumen ecosystem and thus our work has focused on developing a model that accounts for the specificities of the fermentation performed by the rumen microbiota. To expand the capabilities of our model, it is of course needed to provide a mathematical description of the rumen environment and of the input and output fluxes of the rumen as it has been included in existing models (Baldwin et al., 1987; Dijkstra et al., 1992). We think that the mathematical structure developed here can facilitate the standardization of rumen models, which is central to boost further modelling progresses and favour exchange between rumen modellers. In addition, incorporation of new aspects on rumen function into mechanistic models can complexify existing rumen models. Given the different time scales of processes involved in rumen metabolism and their non-linear nature, adequate and robust software is required to provide numerically stable simulations. Matlab® and the free software Scilab (`http://www.scilab.org/fr`) are excellent options due to their numerical and functional capabilities.

4.1. Parameter estimation strategy

The strategy that we used to estimate the parameters of the model aimed to reduce the number of parameters specific to each treatment combination to render possible the identification of the most sensitive parameters. A large body of knowledge on rumen fermentation was incorporated into the strategy via the setting of prior values or by relationships such as the biochemistry of sugars and amino acids fermentation. This approach facilitates the numerical issues related to the optimization problem. In addition, we avoid known difficulties associated with high correlation between the parameters of the Monod kinetics. This correlation is reflected by the fact that is often possible to

accurately estimate the ratio $k_{\mathrm{m},j}/K_{\mathrm{s},j}$, but not to accurately estimate the individual parameters (Holmberg, 1982).

The strategy used is not only suitable for handling numerical issues but also produces outcomes that have a clear biological interpretation. For instance, the experimental study of (Serment et al., 2016) identified the effect of the inoculum as the most influential factor of the fermentation pattern. This effect is reflected by the results of the parameter estimation. The estimated parameters of each treatment combination indicated that the fluxes distribution for sugars utilization depended mainly on the inoculum. However, it is important to keep in mind that the effect of the inoculum is modulated by the substrate via microbial adaptation (Broudiscou et al., 2014).

4.2. Stoichiometry and pathways of rumen fermentation

Stoichiometry is a central aspect of any fermentation model. Empirical approaches have been essentially developed to describe in particular the stoichiometry of VFA in the rumen by deriving equations from the analysis of databases that link the proportion of VFA with respect to measured values of composition and digestion of various diets (Friggens et al., 1998; Nozière et al., 2011). For instance, Nozière et al. (2011) used *in vivo* measurements of ruminal VFA production rate, rates of duodenal and faecal digestion to establish empirical equations that predicts the proportion of VFA by using as predictor variables dry matter intake, digestible organic matter, digestible NDF and rumen starch digestibility. By including biochemical stoichiometric relationships, the work of Murphy et al. (1982) established an important basis to estimate empirically the stoichiometric coefficients of VFA produced during rumen fermentation for distinct substrates. By following the work of Murphy et al. (1982), Bannink et al. (2006) developed a stoichiometry model with the attempt of improving the accuracy of prediction of VFA molar proportions in the rumen of lactating cows.

The approach that we have used in the present model aimed to improve the mechanistic representation of the stoichiometry. The formalism used here is similar to the approach used by Bannink et al. (2006) with certain differences related to the detail of the biochemical description of the fermentation and the calculation of the yield factors of

the individuals VFA. For example, in the model developed by Bannink et al. (2006), the production of VFAs were set dependent on the rates of utilization of different types of substrates (including polymers). In our model, extracellular hydrolysis and fermentation reactions that occur at intracellular level are split. With this approach, VFA production is dependent only on the utilization of monomers (either sugars or amino acids), which is more biologically consistent, allowing us to explicitly include well known macroscopic reactions of rumen fermentation (Wolin et al., 1997) (Table 4). Further, amino acids utilization is not aggregated into carbohydrate utilization. This particularity of the model allows to consider the specific metabolism of carbohydrates and proteins by the rumen microbiota, which occur via different pathways (*e.g.,* Embden-Meyerhof-Parmas pathway for hexoses, and Stickland or non-Stickland reactions for amino acids). These pathways exhibit different thermodynamic responses with respect to hydrogen concentration as discussed by Janssen (2010). Taking together, by incorporating a microbial group of amino acids utilizers, our model structure should facilitate the study of alternatives for reducing amino acid deamination, which is of great interest to favour protein utilization by the host animal. It should be said however that the stoichiometry for amino acid fermentation used in our model is an approximation and further refinements are needed to improve the representation of amino acid fermentation. For example, we considered alfalfa as the only source of amino acids in the calculations. However, as it can be seen from Table 1 other components of the feed are source of amino acids and should also be considered. In addition to the weight associated with the amino acid composition of the feed (Ramsay and Pullammanappallil, 2001), the overall stoichiometry and kinetics are weighing by the relative activity of the proteolytic microbes and their substrate affinity (Monod constant). In our model, it is implicitly assumed that the microbiota do not have a particular preference for the amino acids. However, rumen microbes do exhibit different affinities with respect to individual amino acids (Wallace et al., 1997; Bach et al., 2005). As discussed by Wallace et al. (1997), amino acid fermentation could be carried out by either numerically abundant bacteria with low deaminative activity or by few species with high deaminative activity. In our model, we elaborated on the latter option. However, it will be interesting in the future to support our choice on microbiological data of abundance and activity of

amino acids utilizers. With respect to sugars utilization, in our model the stoichiometry is based on the metabolism of hexoses. To consider the metabolism of monosaccharides with five carbon atoms, a generalised method has been proposed by García-Gen et al. (2013). The approach consists in expressing the stoichiometry of the alternative substrate (*e.g.*, xylose) in terms of equivalent glucose fermentation, and assign to the sugars-utilizers group the capability of growing with multiple substrates. The kinetic parameters and microbial yields are set to be dependent on each type of substrate. The kinetics of utilization include a competitive inhibition term among the multiple substrates.

With respect to hydrogen and methane, existing rumen models based on the work of Baldwin et al. (1987) and Dijkstra et al. (1992), use the same approach for predicting methane production. This approach consists in calculating stoichiometrically the methane from the net surplus of hydrogen in the rumen, which is obtained from subtracting the hydrogen used for microbial growth and biohydrogenation to the hydrogen production from fermentation. This approach does not consider the effect of the methanogen population nor the effect of liquid-gas transfer phenomena. By including these aspects, our model contributes to the mechanistic representation of ruminal hydrogen and methane. Moreover, our model complements recent modelling attempts to improve the representation of hydrogen metabolism and methane production in the rumen (Vetharaniam et al., 2015; Wang et al., 2016).

By incorporating fermentation reactions, we are not only able to predict H_2 and CH_4 as other models do (Mills et al., 2001), but also to maintain elementary balances of nitrogen and carbon. Furthermore, by taking into account NH_3 and CO_2, our model allows linking of fermentation products with the pH via the definition of acid-base reactions, as it will be discussed later on. In our approach, the yield factors are parameterized to be dependent on the flux distribution (defined by the parameters λ_i) across the set of reactions defined in the model. In the current version of the model, we used fixed stoichiometric yields. Nevertheless, the yields (and the repartition of fluxes) depends partly on thermodynamics and may vary. For instance, hydrogen concentration is linked to the fermentation pattern and shift of reactions (Offner and Sauvant, 2006; Janssen, 2010). This thermodynamic driving force results in a variable stoichiometry (Rodríguez

et al., 2006). Including thermodynamic control into the model is indeed a challenging perspective. It should be a useful approach for tackling aspects related to the individual variability of rumen fermentation patterns. We expect that the structure of the model will enable us to include in the future such aspects.

Fermentation was represented in aggregated form. It may be also interesting to relax the level of aggregation to consider for instance lactate metabolism and address aspects concerning lactic acidosis state (Mills et al., 2014). In this direction, the kinetic model developed by Muñoz-Tamayo et al. (2011) to describe lactate utilization by human colonic microbiota can be integrated in the model here developed.

Currently, our representation of the fermentation pathway includes three theoretical functional groups of microbes with fixed chemical composition. This approach differs from the one often used in rumen models where the microbiota is represented either by a single microbial group (Baldwin et al., 1987) or by two microbial pools, namely fibre degraders and starch degraders (Dijkstra et al., 1992). In our model, the functional groups are defined solely in terms of the monomers sugars, amino acids and hydrogen used as substrates. This approach is a clearly simplified representation of the rumen microbiome, which for example ignores variation of the chemical composition of rumen microbiota that has been suggested to affect the fermentation (Dijkstra et al., 1992). In our model structure, the actions of protozoa are included in an aggregated way by considering that sugars and amino acids utilizers account for the combined activity of both bacteria and protozoa. The engulfment of bacteria is incorporated by considering a kinetics of cell death. Given the strong link between protozoa concentration and methane production (Guyader et al., 2014), it will be interesting to including explicitly this microbial group as in the model of Dijkstra (1994).

In the present version of our model, we do not include explicitly maintenance requirements of rumen microbes. Under the experimental conditions here studied, maintenance requirements were assumed to be negligible. Indeed, the model performance was satisfactory without including this factor. However, under *in vivo* conditions, microbial maintenance can be very high. Including maintenance is therefore central and thus should be included in the model. It should be noted that including a maintenance term by using

for example the Pirt equation into our model can be done straightforward. To favour a mechanistic representation of microbial metabolism, mechanistic modelling of maintenance is a challenging subject that calls for re-evaluation of previous models (including the Pirt equation). An ideal model should explicitly describe the different non-growth components that constitute microbial maintenance as discussed by van Bodegom (2007).

It is clear that further improvements are needed to gain insight into the full picture of the rumen microbiome. However, it should be said that the approach used here and the simplifications adopted already provide a satisfactory prediction of the fermentation pattern.

4.3. A mechanistic modelling of pH

Our model satisfactorily represented the dynamics of pH for the four treatment combinations analyzed. Nevertheless, in this experiment the pH varied in a narrow range due to the high buffering capacity of the medium. To validate our model, it will be necessary to compare the model against experimental data exhibiting pH variations in a broader range than the one analyzed here.

The mechanistic description of pH is one of the hallmarks of the present model. The formulation of acid-base equilibrium reactions of the main chemical components that influence the pH enhances the knowledge basis of the model. We have integrated acid-base equilibria to the liquid-gas transfer of CO_2, and the fermentation pattern (VFA, NH_3), extending previous attempts to model pH (Imamidoost and Cant, 2005). The model developed here follows the principle of considering the bicarbonate system of the rumen as an open system (Kohn and Dunlap, 1998; Hille et al., 2016)). Although our model does not yet incorporate the role of salivary secretion, VFA absorption on rumen fermentation, and other phenomena that play a role on the buffer capacity of the rumen. It will also be important to incorporate the retroactive effect of the pH on the fermentation (Argyle and Baldwin, 1988) and microbial activities. The current model structure should facilitate such development.

Finally, since the model was calibrated with a small number of experiments, further validation with independent data is required. In this line, the next step of our work will be to

challenge the model against other data set with different substrates to assess how model parameters vary with respect the substrate type. Furthermore, we will extend the developed model for describing *in vitro* continuous systems (RUSITEC and chemostat) that accounts for substrate inflows and products outflows. Validation of the model structure for *in vitro* continuous systems will then support the task of modelling the rumen under *in vivo* conditions, which is the ultimate goal of our modelling endeavour. For this, further extensions are required to account for physiological factors such as kinetics of substrate supply, VFA and NH_3 absorption. Since, the physical form of the feeds impacts transit time and nutrient availability, it will be useful to include this aspect in a further version. Incorporating the aforementioned factors into the model should improve its capabilities for both research and practical purposes such as the design of optimal nutritional strategies .

5. Conclusions

A mechanistic mathematical model of *in vitro* rumen fermentation has been developed. The model was calibrated with experimental data and represented effectively the profile of individuals VFA, pH, NH_3 and gas production (H_2, CO_2, CH_4). By enhancing the description of microbial metabolism, acid-base reactions (central for pH calculation) and gas-liquid transfer, this model contributes to improve mechanistic modelling of rumen fermentation. It also provides a strong basis for extension to modelling *in vivo* fermentation.

Acknowledgements

Special thanks to Nicolas Friggens (INRA-AgroParisTech, UMR 791 Modélisation Systémique Appliquée aux Ruminants, Paris, France) for improving the English language and the readability of the manuscript. We thank the technical staff of the experimental farm at Thiverval-Grignon, whose work contributes to the generation of useful data for model developments. We would like to thank the three anonymous reviewers whose critical feedback helped to greatly improve this manuscript.

References

Alemu, A. W., Dijkstra, J., Bannink, A., France, J., Kebreab, E., 2011. Rumen stoichiometric models and their contribution and challenges in predicting enteric methane production. Anim. Feed Sci. Technol. 166, 761–778.

Argyle, J., Baldwin, R., 1988. Modeling of rumen water kinetics and effects on rumen pH changes. J. Dairy Sci. 78, 1178–1188.

Atasoglu, C., Newbold, C. J., Wallace, R. J., 2001. Incorporation of [^{15}N] ammonia by the cellulolytic ruminal bacteria *Fibrobacter succinogenes* BL2, *Ruminococcus albus* SY3, and *Ruminococcus flavefaciens* 17. Appl Environ Microbiol 67, 2819–2822.

Bach, A., Calsamiglia, S., Stern, M. D., 2005. Nitrogen metabolism in the rumen. J Dairy Sci 88 Suppl 1, E9–21.

Baldwin, R. L., Denham, S. C., 1979. Quantitative and dynamic aspects of nitrogen metabolism in the rumen: a modeling analysis. J Anim Sci 49, 1631–1639.

Baldwin, R. L., Thornley, J. H., Beever, D. E., 1987. Metabolism of the lactating cow. II. Digestive elements of a mechanistic model. J. Dairy Res. 54, 107–131.

Bannink, A., Kogut, J., Dijkstra, J., France, J., Kebreab, E., Van Vuuren, A. M., Tamminga, S., 2006. Estimation of the stoichiometry of volatile fatty acid production in the rumen of lactating cows. J. Theor Biol. 238, 36–51.

Bannink, A., Van Schijndel, M., Dijkstra, J., 2011. A model of enteric fermentation in dairy cows to estimate methane emission for the Dutch National Inventory Report using the IPCC Tier 3 approach. Anim. Feed Sci. Technol. 166, 603–618.

Batstone, D. J., Keller, J., Angelidaki, I., Kalyuzhnyi, S. V., Pavlostathis, S. G., Rozzi, A., Sanders, W. T., Siegrist, H., Vavilin, V. A., 2002. Anaerobic Digestion Model No.1 (ADM1). IWA Publishing, London.

Broudiscou, L. P., Offner, A., Sauvant, D., 2014. Effects of inoculum source, pH, redox potential and headspace di-hydrogen on rumen *in vitro* fermentation yields. Animal 8, 931–937.

Dijkstra, J., 1994. Simulation of the dynamics of protozoa in the rumen. Br J Nutr 72, 679–699.

Dijkstra, J., Ellis, J., Kebreab, E., Strathe, A., López, S., France, J., Bannink, A., 2012. Ruminal pH regulation and nutritional consequences of low pH. Anim. Feed Sci. Technol. 172, 22–33.

Dijkstra, J., Neal, H. D., Beever, D. E., France, J., Nov 1992. Simulation of nutrient digestion, absorption and outflow in the rumen: model description. J. Nutr. 122, 2239–2256.

Ellis, J., Dijkstra, J., Kebreab, E., Bannink, A., Odongo, N., McBride, B., France, J., 2008. Aspects of rumen microbiology central to mechanistic modelling of methane production in cattle. J. Agric. Sci. 146, 213–233.

Friggens, N., Oldham, J., Dewhurst, R., Horgan, G., 1998. Proportions of volatile fatty acids in relation to the chemical composition of feeds based on grass silage. J. Dairy Sci. 81, 1331–1344.

García-Gen, S., Lema, J. M., Rodríguez, J., 2013. Generalised modelling approach for anaerobic co-digestion of fermentable substrates. Bioresour Technol 147, 525–533.

Giger-Reverdin, S., Serment, A., Sauvant, D., 2014. Evaluation of a mechanistic model simulating *in vitro* gas production and ammonia evolution for a variety of feedstuffs fed to ruminants. In: 8th International Workshop on Modelling Nutrient Digestion and Utilization in Farm Animals, Cairns, Australia.

Guyader, J., Eugène, M., Nozière, P., Morgavi, D. P., Doreau, M., Martin, C., 2014. Influence of rumen protozoa on methane emission in ruminants: a meta-analysis approach. Animal 8, 1816–1825.

Hille, K. T., Hetz, S. K., Rosendahl, J., Braun, H.-S., Pieper, R., Stumpff, F., 2016. Determination of henry's constant, the dissociation constant, and the buffer capacity of the bicarbonate system in ruminal fluid. J Dairy Sci 99, 369–385.

Holmberg, A., 1982. On the practical identifiability of microbial growth models incorporating Michaelis-Menten type nonlinearities. Math. Biosci. 62, 23–43.

Imamidoost, R., Cant, J. P., 2005. Non-steady-state modeling of effects of timing and level of concentrate supplementation on ruminal pH and forage intake in high-producing, grazing ewes. J. Anim Sci. 83, 1102–1115.

Janssen, P. H., 2010. Influence of hydrogen on rumen methane formation and fermentation balances through microbial growth kinetics and fermentation thermodynamics. Anim. Feed Sci. Technol. 160, 1–22.

Kohn, R., Boston, R., 2000. The role of thermodynamics in controlling rumen metabolism. In: McNamara, J., France, J., Beever, D. (Eds.), Modelling Nutrient Utilization in Farm Animals. CAB International, Wallingford, UK. pp. 11–24.

Kohn, R. A., Dunlap, T. F., 1998. Calculation of the buffering capacity of bicarbonate in the rumen and *in vitro*. J. Anim Sci. 76, 1702–1709.

Krause, D. O., Russell, J. B., 1996. An rRNA approach for assessing the role of obligate amino acid-fermenting bacteria in ruminal amino acid deamination. Appl Environ Microbiol 62, 815–821.

Lagarias, J. C., Reeds, J. A., Wright, M. H., Wright, P. E., 1998. Convergence properties of the Nelder-Mead simplex method in low dimensions. SIAM J. Optim. 9, 112–147.

Lescoat, P., Sauvant, D., 1995. Development of a mechanistic model for rumen digestion validated using the duodenal flux of amino acids. Reprod. Nutr. Dev. 35, 45–70.

Lin, L. I.-K., 1989. A concordance correlation coefficient to evaluate reproducibility. Biometrics, 255–268.

Maaroufi, C., Chapoutot, P., Sauvant, D., Giger-Reverdin, S., 2009. Fractionation of pea flour with pilot scale sieving. II. *In vitro* fermentation of pea seed fractions of different particle sizes. Anim. Feed Sci. Technol. 154, 135–150.

Menke, K., Raab, L., Salewski, A., Steingass, H., Fritz, D., Schneider, W., 1979. The estimation of the digestibility and metabolizable energy content of ruminant feedingstuffs from the gas production when they are incubated with rumen liquor in vitro. J. Agric. Sci. 93, 217–222.

Mills, J. A., Dijkstra, J., Bannink, A., Cammell, S. B., Kebreab, E., France, J., 2001. A mechanistic model of whole-tract digestion and methanogenesis in the lactating dairy cow: model development, evaluation, and application. J. Anim. Sci. 79, 1584–1597.

Mills, J. A. N., Crompton, L. A., Ellis, J. L., Dijkstra, J., Bannink, A., Hook, S., Benchaar, C., France, J., 2014. A dynamic mechanistic model of lactic acid metabolism in the rumen. J. Dairy Sci. 97, 2398–2414.

Morgavi, D. P., Forano, E., Martin, C., Newbold, C. J., 2010. Microbial ecosystem and methanogenesis in ruminants. Animal 4, 1024–1036.

Motelica-Wagenaar, A. M., Nauta, A., van den Heuvel, E. G. H. M., Kleerebezem, R., 2014. Flux analysis of the human proximal colon using anaerobic digestion model 1. Anaerobe 28, 137–148.

Muñoz-Tamayo, R., Laroche, B., Leclerc, M., Walter, E., 2009. IDEAS: a parameter identification toolbox with symbolic analysis of uncertainty and its application to biological modelling. In: Prepints of the 15th IFAC Symposium on System Identification, Saint-Malo, France. pp. 1271–1276.
URL `http://www.inra.fr/miaj/public/logiciels/ideas/index.html`

Muñoz-Tamayo, R., Laroche, B., Walter, E., Dore, J., Duncan, S. H., Flint, H. J., Leclerc, M., 2011. Kinetic modelling of lactate utilization and butyrate production by key human colonic bacterial species. FEMS Microbiol Ecol 76, 615–624.

Muñoz-Tamayo, R., Laroche, B., Walter, E., Dore, J., Leclerc, M., 2010. Mathematical modelling of carbohydrate degradation by human colonic microbiota. J. Theor Biol. 266, 189–201.

Murphy, M. R., Baldwin, R. L., Koong, L. J., 1982. Estimation of stoichiometric parameters for rumen fermentation of roughage and concentrate diets. J. Anim. Sci. 55, 411–421.

Nagadi, S., Herrero, M., Jessop, N., 2000. The influence of diet of the donor animal on the initial bacterial concentration of ruminal fluid and in vitro gas production degradability parameters. Animal Feed Science and Technology 87 (3), 231–239.

Nozière, P., Glasser, F., Sauvant, D., 2011. In vivo production and molar percentages of volatile fatty acids in the rumen: a quantitative review by an empirical approach. Animal 5, 403–414.

Offner, A., Sauvant, D., 2004. Comparative evaluation of the Molly, CNCPS, and LES rumen models. Anim. Feed Sci. Technol. 112 (1), 107–130.

Offner, A., Sauvant, D., 2006. Thermodynamic modeling of ruminal fermentations. Anim. Res. 55, 343–365.

Petersen, E. E., 1965. Chemical reaction analysis. Prentice Hall, Englewood Cliffs, New Jersey.

Piñeiro, G., Perelman, S., Guerschman, J. P., Paruelo, J. M., 2008. How to evaluate models: observed vs. predicted or predicted vs. observed? Ecological Modelling 216 (3), 316–322.

Ramsay, I. R., Pullammanappallil, P. C., 2001. Protein degradation during anaerobic wastewater treatment: derivation of stoichiometry. Biodegradation 12 (4), 247–257.

Reichl, J. R., Baldwin, R. L., 1975. Rumen modeling: rumen input-output balance models. J. Dairy Sci. 58, 879–890.

Robinson, J. A., Tiedje, J. M., 1982. Kinetics of hydrogen consumption by rumen fluid, anaerobic digestor sludge, and sediment. Appl. Environ. Microbiol. 44, 1374–1384.

Rodríguez, J., Lema, J. M., van Loosdrecht, M. C. M., Kleerebezem, R., 2006. Variable stoichiometry with thermodynamic control in ADM1. Wat. Sci. Technol. 54, 101–110.

Rosen, C., Vrecko, D., Gernaey, K. V., Pons, M. N., Jeppsson, U., 2006. Implementing ADM1) for plant-wide benchmark simulations in matlab/simulink. Wat. Sci. Technol. 54, 11–19.

Russell, J. B., Wallace, R. J., 1997. Energy-yielding and energy-consuming reactions. In: Hobson, P., Stewart, C. S. (Eds.), The rumen microbial ecosystem, 2nd Edition. Chapman & Hall, London, UK., pp. 246–282.

Sari, T., Harmand, J., May 2016. A model of a syntrophic relationship between two microbial species in a chemostat including maintenance. Math Biosci 275, 1–9.

Serment, A., 2012. Pattern and extent of ruminal biotransformation (chapter 3). Ph.D. thesis, AgroParisTech.

Serment, A., Giger-Reverdin, S., Schmidely, P., Dhumez, O., Broudiscou, L. P., Sauvant, D., 2016. *In vitro* fermentation of total mixed diets differing in concentrate proportion: relative effects of inocula and substrates. J Sci Food Agric 96, 160–168.

Serment, A., Sauvant, D., 2011. A mechanistic model of pH and gas exchanges in the rumen and its *in vitro* application. In: Sauvant, D., Van Milgen, J., Faverdin, P., Friggens, N. (Eds.), Modelling nutrient digestion and utilisation in farm animals. Wageningen Academic Publishers, pp. 148–157.

Serment, A., Schmidely, P., Giger-Reverdin, S., Chapoutot, P., Sauvant, D., Aug 2011. Effects of the percentage of concentrate on rumen fermentation, nutrient digestibility, plasma metabolites, and milk composition in mid-lactation goats. J Dairy Sci 94 (8), 3960–3972.

Shampine, L. F., Reichelt, M. W., 1997. The Matlab ODE suite. SIAM J. Sci. Comput. 18, 1–22.

van Bodegom, P., May 2007. Microbial maintenance: a critical review on its quantification. Microb Ecol 53 (4), 513–523.

Vetharaniam, I., Vibart, R. E., Hanigan, M. D., Janssen, P. H., Tavendale, M. H., Pacheco, D., 2015. A modified version of the Molly rumen model to quantify methane emissions from sheep. J. Anim Sci. 93, 3551–3563.

Waldo, D. R., Smith, L. W., Cox, E. L., 1972. Model of cellulose disappearance from the rumen. J. Dairy Sci. 55, 125–129.

Wallace, R. J., Onodera, R., Cotta, M. A., 1997. Metabolism of nitrogen-containing compounds. In: Hobson, P., Stewart, C. S. (Eds.), The rumen microbial ecosystem, 2nd Edition. Chapman & Hall, London, UK., pp. 283–328.

Walter, E., Pronzato, L., 1997. Identification of Parametric Models from Experimental Data. Springer, London.

Wang, M., Wang, R., Janssen, P. H., Zhang, X. M., Sun, X. Z., Pacheco, D., Tan, Z. L., 2016a. Sampling procedure for the measurement of dissolved hydrogen and volatile fatty acids in the rumen of dairy cows. J Anim Sci 94, 1159–1169.

Wang, Y., Janssen, P. H., Lynch, T. A., van Brunt, B., Pacheco, D., 2016. A mechanistic model of hydrogen-methanogen dynamics in the rumen. Journal of theoretical biology.

Wolin, M. J., Miller, T. L., Stewart, C. S., 1997. Microbe-microbe interactions. In: Hobson, P., Stewart, C. S. (Eds.), The rumen microbial ecosystem, 2nd Edition. Chapman & Hall, London, UK., pp. 467–491.

Xu, A., Dolfing, J., Curtis, T. P., Montague, G., Martin, E., 2011. Maintenance affects the stability of a two-tiered microbial 'food chain'? Journal of theoretical biology 276, 35–41.

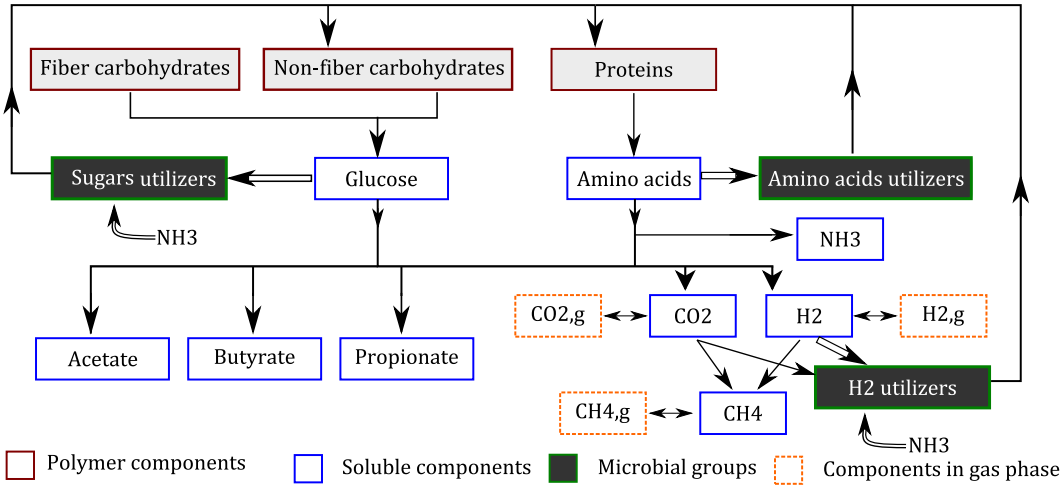

Figure 1: Fluxes representing the digestion of feedstuffs by the rumen microbiota. Hydrolysis of carbohydrates (fiber and non-fiber) and proteins releases respectively sugars and amino acids monomers, which are further utilized by the microbiota intracellularly. The utilization of substrate occurs via by two processes, namely product formation (single arrows) and microbial growth (double arrows). The metabolic fluxes of substrate utilization are thus partitioned in these two processes. The utilization of each substrate is attributed to a single microbial functional group. Microbial synthesis requires both carbon and nitrogen. Dead microbial cells are recycled as source of non-fibers carbohydrates and proteins. CO_2, CH_4 and H_2 produced during fermentation participate in liquid-gas transfer phenomena.

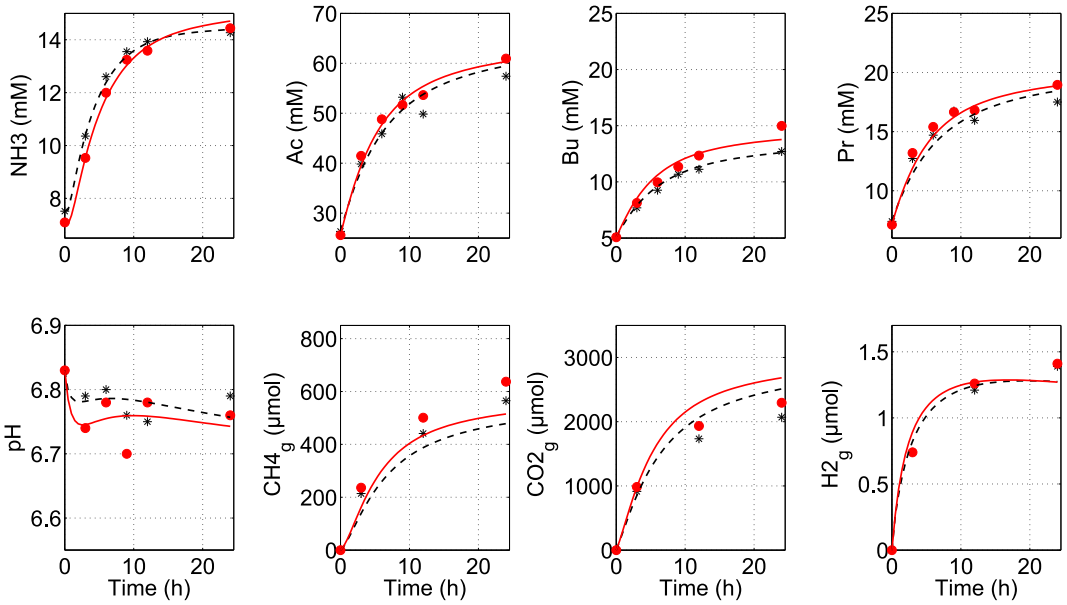

Figure 2: Model calibration with experimental data using the inoculum (L_i) adapted to the low concentrate . The experimental data of the treatments with low concentrate substrate (L_iL_s (*)) and high substrate concentrate (L_iH_s (•)) are compared against the model responses depicted in dashed lines (L_iL_s) and solid lines (L_iH_s).

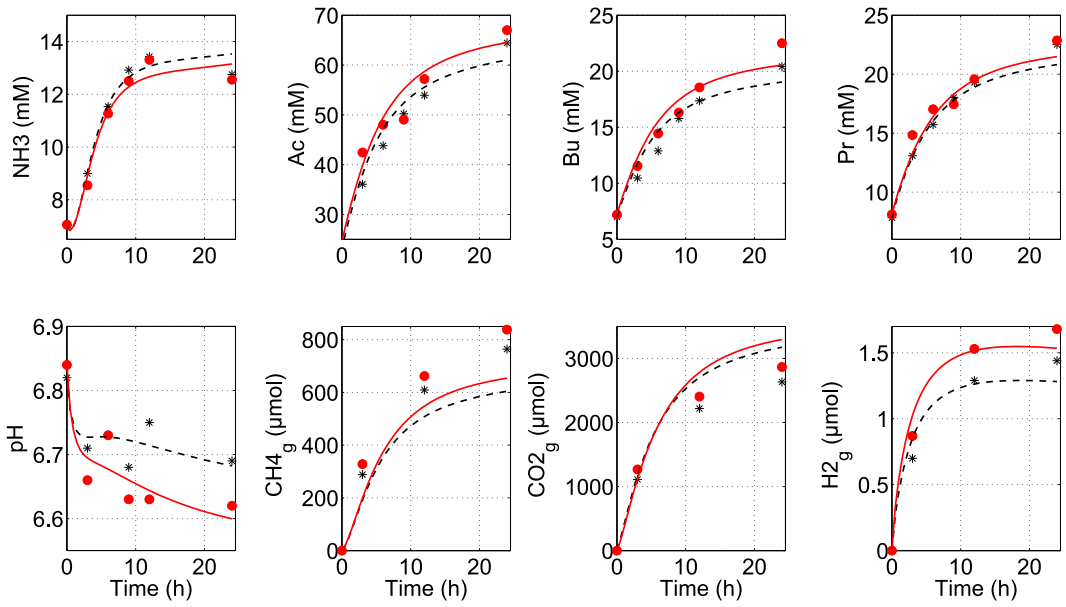

Figure 3: Model calibration with experimental data using the inoculum (H_i) adapted to the high concentrate. The experimental data of the treatments with low concentrate substrate (H_iL_s (*)) and high concentrate substrate (H_iH_s (•)) are compared against the model responses depicted in dashed lines (H_iL_s) and solid lines (H_iH_s).

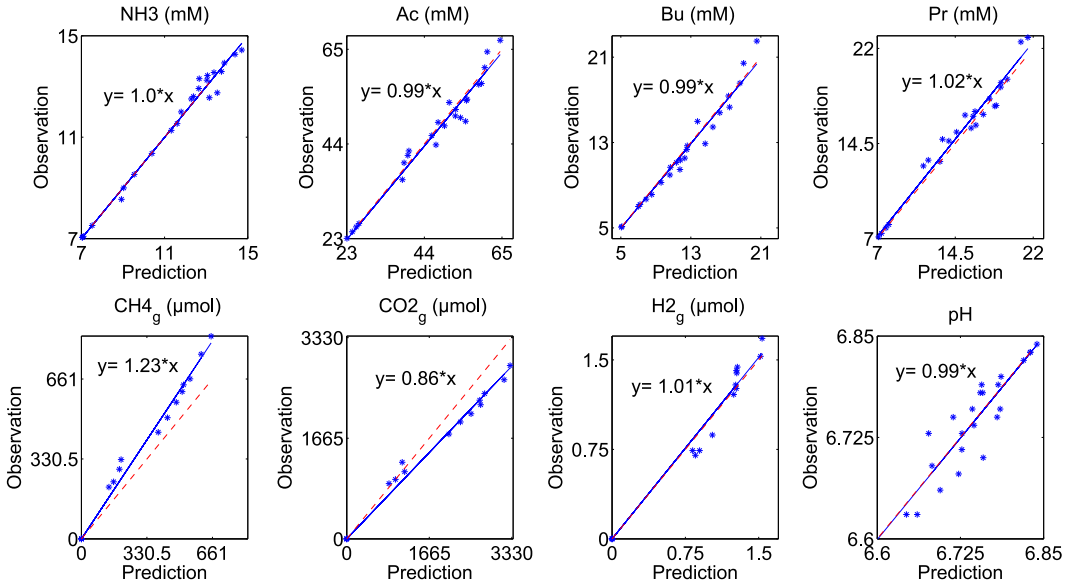

Figure 4: The observations are plot against the model predictions (*). The linear fitted curve is displayed in solid line with the resulting regression equation. The line $y = x$ is shown in dashed line. The linearity between model outputs and observations indicates the reliability of the mathematical model to represent the pattern of rumen fermentation.

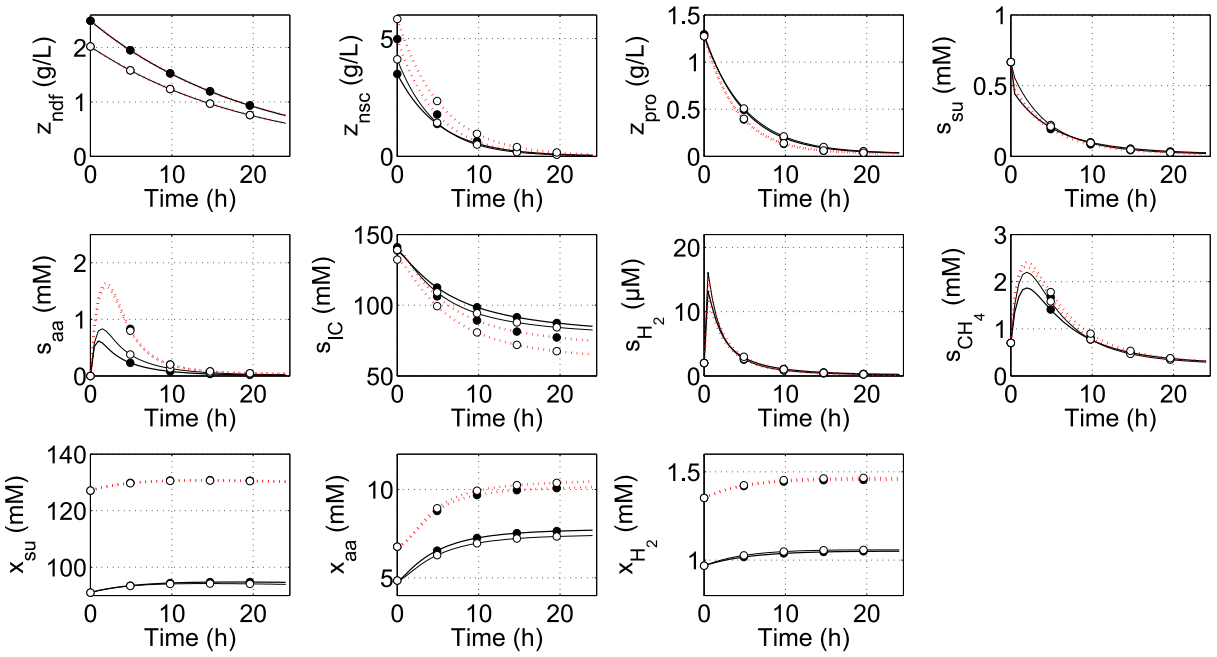

Figure 5: Predicted dynamics of non measured variables for the treatment combinations. Solid lines refer to the inoculum L_i adapted to the low concentrate diet. Dotted lines refer to the inoculum H_i adapted to the high concentrate diet. Filled circles refer to the low concentrate substrate L_s. Open circles refer to the high concentrate substrate H_s. The variables are neutral detergent fiber concentration (z_{ndf}), non-structural carbohydrates concentration (z_{nsc}), protein concentration (z_{pro}), sugars concentration (s_{su}), average amino acids concentration (s_{aa}), concentration of inorganic carbon (s_{IC}), dissolved hydrogen concentration ($s_{\mathrm{H_2}}$) and dissolved methane concentration ($s_{\mathrm{CH_4}}$), concentration of sugars-utilizing microbes (x_{su}), concentration of amino acids-utilizing microbes (x_{aa}), and concentration of hydrogen-utilizing microbes($x_{\mathrm{H_2}}$).

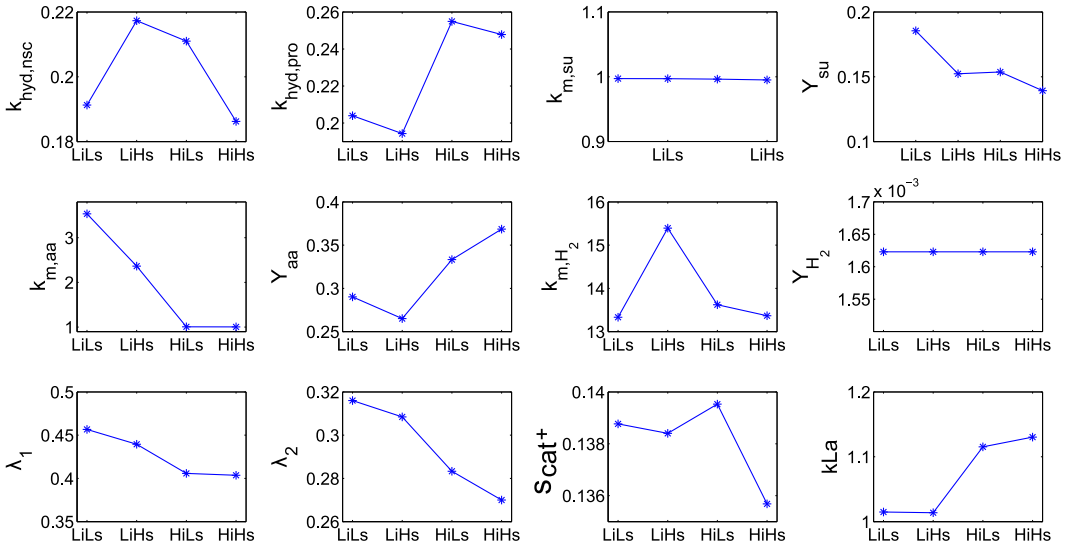

Figure 6: Estimated parameters for each treatment combination.

Table 1: Composition of the substrates (Serment, 2012)

		L substrate	H substrate
Ingredients (100× g/g of DM)			
Forage		65	30
	Grass hay	29.9	13.8
	Dehydrated alfalfa[a]	35.1	16.2
Concentrate		35	70
	Commercial concentrate[b]	20	50
	Sugar beet pulp silage	7	20
	Calcium palm oil salt	1.4	
	Soybean meal	6.6	
Chemical composition (100× g/g of DM)			
Crude protein		14.4	14.1
aNDFom[c]		40.5	32.6
ADFom[d]		23.0	18.0
Lignin		3.12	2.30
Starch		4.39	9.39
Ash		8.40	7.05
Fatty acids		2.35	2.55

[a] Rumiluz, Désialis, Paris (France).

[b] Agralys Aliment, Châteaudun (France): 18% maize, 14% sugar beet pulp, 12% sunflower meal, 10% wheat, 10% soybean, 9% rapeseed meal, 6% soybean meal, 4% wheat distiller, 3.5% linseed, 3% pea seed, 1% rapeseed oil, 3% molasses, 6.5% mineral and vitamin premix.

[c] aNDFom: Neutral Detergent Fiber assayed with a heat stable amylase and expressed exclusive of residual ash.

[d] ADFom: Acid Detergent Fiber expressed exclusive of residual ash.

Table 2: Model notation and abbreviations.

	Definition	Units
Abbreviations		
NSC	Non-structural carbohydrates	
NDF	Neutral detergent fiber	
VFA	Volatile fatty acids	
Model variables		
	Polymer components	
z_{ndf}	Neutral detergent fiber (NDF) concentration	g/L
z_{nsc}	Non-structural carbohydrates (NSC) concentration	g/L
z_{pro}	Proteins concentration	g/L
Soluble components		
s_{su}	Sugars concentration	mol/L
s_{aa}	Average amino acids concentration	mol/L
s_{ac}	Total acetate concentration	mol/L
s_{bu}	Total butyrate concentration	mol/L
s_{pr}	Total propionate concentration	mol/L
s_{VFA}	Total volatile fatty acids concentration	mol/L
s_{IC}	Inorganic carbon concentration	mol/L
$s_{\mathrm{CO_2}}$	Carbon dioxide concentration in the liquid phase	mol/L
s_{IN}	Inorganic nitrogen concentration	mol/L
$s_{\mathrm{NH_3}}$	Ammonia concentration	mol/L
$s_{\mathrm{H_2}}$	Hydrogen concentration in liquid phase	mol/L
$s_{\mathrm{CH_4}}$	Methane concentration in the liquid phase	mol/L
Gas components		
$n_{\mathrm{g,H_2}}$	Moles of hydrogen in the gas phase	mol
$n_{\mathrm{g,CO_2}}$	Moles of carbon dioxide in the gas phase	mol
$n_{\mathrm{g,CH_4}}$	Moles of methane in the gas phase	mol
Microbial functional groups		
x_{su}	Concentration of sugars-utilizing microbes	mol/L
x_{aa}	Concentration of amino acids-utilizing microbes	mol/L
$x_{\mathrm{H_2}}$	Concentration of hydrogen-utilizing microbes (methanogens)	mol/L
Acid-base components		
$s_{\mathrm{cat+}}$	Concentration of metallic cations	mol/L
$s_{\mathrm{NH_4^+}}$	Ammonium ions concentration	mol/L
$s_{\mathrm{H+}}$	Hydrogen ions concentration	mol/L
$s_{\mathrm{HCO_3^-}}$	Bicarbonate concentration	mol/L
$s_{\mathrm{ac-}}$	Acetate ions concentration	mol/L
$s_{\mathrm{bu-}}$	Butyrate ions concentration	mol/L
$s_{\mathrm{pr-}}$	Propionate ions concentration	mol/L
$s_{\mathrm{VFA-}}$	Total volatile fatty acids ions concentration	mol/L
s_{hac}	Acetate concentration in free form	mol/L
s_{hbu}	Butyrate concentration in free form	mol/L
s_{hpr}	Propionate concentration in free form	mol/L

Table 2: Model notation and abbreviations.

	Definition	Units
$s_{\mathrm{hVFA-}}$	Total volatile fatty acids concentration in free form	mol/L
$s_{\mathrm{OH-}}$	Hydroxide ions concentration	mol/L
Rates and parameters		
Rates		
μ_j	Growth rate of the microbial group j	mol j/(L·h)
ρ_j	Kinetic rate of microbial process j	mol (or g) j/(L·h)
ρ_{x_j}	Death cell rate of microbes j	mol j/(L·h)
$\rho_{\mathrm{T},j}$	Liquid-gas transfer rate of component j	mol j/(L·h)
Biochemical parameters		
λ_k	Molar fraction of the sugars utilized via reaction k	mol/mol
$\mu_{\mathrm{max},j}$	Maximum specific growth rate constant of the microbial group j	h^{-1}
$\sigma_{i,\mathrm{aa}}$	Stoichiometric coefficient of component i from amino acids utilization	mol/mol
f_j	Fraction of the substrate j utilized for product formation	mol/mol
$f_{\mathrm{ch,x}}$	Mass fraction of carbohydrates in the microbial cells	g/g
$f_{\mathrm{pro,x}}$	Mass fraction of proteins in the microbial cells	g/g
k_{d}	Death cell rate constant	h^{-1}
$k_{\mathrm{hyd,ndf}}$	Hydrolysis rate constant of cell wall carbohydrates	h^{-1}
$k_{\mathrm{hyd,nsc}}$	Hydrolysis rate constant of non-structural carbohydrates	h^{-1}
$k_{\mathrm{hyd,pro}}$	Hydrolysis rate constant of proteins	h^{-1}
$k_{\mathrm{m,aa}}$	Maximum specific utilization rate constant of amino acids	mol/(mol · h)
$k_{\mathrm{m,H_2}}$	Maximum specific utilization rate constant of hydrogen	mol/(mol · h)
$k_{\mathrm{m,su}}$	Maximum specific utilization rate constant of amino sugars	mol/(mol · h)
$K_{\mathrm{s,aa}}$	Monod constant associated with the utilization of amino acids	mol/L
$K_{\mathrm{s,H_2}}$	Monod constant associated with the utilization of hydrogen	mol/L
$K_{\mathrm{s,su}}$	Monod constant associated with the utilization of sugars	mol/L
$K_{\mathrm{s,IN}}$	Nitrogen limitation constant	mol/L
Y_j	Microbial biomass yield factor	mol/mol
$Y_{i,j}$	Yield factor of the compound i during utilization of substrate j	mol/mol
Physicochemical parameters		
$K_{\mathrm{a,CO_2}}$	Equilibrium constant of bicarbonate	
$K_{\mathrm{a,NH_4}}$	Equilibrium constant of ammonium	
$K_{\mathrm{a,VFA}}$	Equilibrium constant of VFA	
K_w	Equilibrium coefficient of water	
$k_{\mathrm{L}}\mathrm{a}$	Liquid-gas transfer constant	h^{-1}
$K_{\mathrm{H,CO_2}}$	Henry's law coefficient of carbon dioxide	M/bar
$K_{\mathrm{H,CH_4}}$	Henry's law coefficient of methane	M/bar
$K_{\mathrm{H,H_2}}$	Henry's law coefficient of hydrogen	M/bar
P	Pressure	bars
T	Temperature	K
w_j	Molecular weight (MW) of component j	g/mol

Table 2: Model notation and abbreviations.

	Definition	Units
w_{aa}	Molecular weight of average amino acid	g/mol
w_{mb}	Molecular weight of microbial cells	g/mol
w_{su}	Molecular weight of sugars	g/mol
V_l	Volume of the liquid phase	L

Table 3: Petersen matrix representing rumen fermentation. The microbial utilization of substrate j is described by the kinetic rate ρ_j. The elements of the matrix describe the stoichiometry of the fermentation via the yield factors. The utilization of one mole of substrate j produces Y_j moles of microbial cells. $Y_{i,j}$ is the amount of moles of component i that is either consumed or produced by the utilization of one mole of substrate j.

	Component→ i	1	**2**	**3**	**4**	**5**	**6**	**7**	**8**	**Kinetic rate**
j	**Microbial process ↓**	z_{ndf}	z_{nsc}	z_{pro}	s_{su}	s_{aa}	$s_{\mathrm{H_2}}$	s_{ac}	s_{bu}	
1	Hydrolysis of NDF carbohydrates	-1			$1/w_{\mathrm{su}}$					ρ_{ndf}
1	Hydrolysis of NSC carbohydrates		-1		$1/w_{\mathrm{su}}$					ρ_{nsc}
2	Hydrolysis of proteins			-1		1				ρ_{pro}
3	Utilization of sugars				-1		$Y_{\mathrm{H_2,su}}$	$Y_{\mathrm{ac,su}}$	$Y_{\mathrm{bu,su}}$	ρ_{su}
4	Utilization of amino acids					-1	$Y_{\mathrm{H_2,aa}}$	$Y_{\mathrm{ac,aa}}$	$Y_{\mathrm{bu,aa}}$	ρ_{aa}
5	Utilization of hydrogen						-1			$\rho_{\mathrm{H_2}}$
6	Death of sugars utilizers		$f_{\mathrm{ch,x}} \cdot w_{\mathrm{mb}}$	$f_{\mathrm{pro,x}} \cdot w_{\mathrm{mb}}$						$\rho_{x_{\mathrm{su}}}$
7	Death of amino acids utilizers		$f_{\mathrm{ch,x}} \cdot w_{\mathrm{mb}}$	$f_{\mathrm{pro,x}} \cdot w_{\mathrm{mb}}$						$\rho_{x_{\mathrm{aa}}}$
8	Death of hydrogen utilizers		$f_{\mathrm{ch,x}} \cdot w_{\mathrm{mb}}$	$f_{\mathrm{pro,x}} \cdot w_{\mathrm{mb}}$						$\rho_{x_{\mathrm{H_2}}}$

	Component→ i	**9**	**10**	**11**	**12**	**13**	**14**	**15**	**Kinetic rate**
j	**Microbial process ↓**	s_{pr}	s_{IN}	s_{IC}	$s_{\mathrm{CH_4}}$	x_{su}	x_{aa}	$x_{\mathrm{H_2}}$	
1	Hydrolysis of NDF carbohydrates								$\rho_{\mathrm{ndf}} = k_{\mathrm{hyd,ndf}} \cdot z_{\mathrm{ndf}}$
1	Hydrolysis of NSC carbohydrates								$\rho_{\mathrm{nsc}} = k_{\mathrm{hyd,nsc}} \cdot z_{\mathrm{nsc}}$
2	Hydrolysis of proteins								$\rho_{\mathrm{pro}} = k_{\mathrm{hyd,pro}} \cdot z_{\mathrm{pro}}$
3	Utilization of sugars	$Y_{\mathrm{pr,su}}$	$Y_{\mathrm{IN,su}}$	$Y_{\mathrm{IC,su}}$		Y_{su}			$\rho_{\mathrm{su}} = k_{\mathrm{m,su}} \frac{s_{\mathrm{su}}}{K_{\mathrm{s,su}} + s_{\mathrm{su}}} x_{\mathrm{su}} \cdot I_{\mathrm{IN}}$
4	Utilization of amino acids	$Y_{\mathrm{pr,aa}}$	$Y_{\mathrm{IN,aa}}$	$Y_{\mathrm{IC,aa}}$			Y_{aa}		$\rho_{\mathrm{aa}} = k_{\mathrm{m,aa}} \frac{s_{\mathrm{aa}}}{K_{\mathrm{s,aa}} + s_{\mathrm{aa}}} x_{\mathrm{aa}}$
5	Utilization of hydrogen		$Y_{\mathrm{IN,H_2}}$	$Y_{\mathrm{IC,H_2}}$	$Y_{\mathrm{CH_4,H_2}}$			$Y_{\mathrm{H_2}}$	$\rho_{\mathrm{H_2}} = k_{\mathrm{m,H_2}} \frac{s_{\mathrm{H_2}}}{K_{\mathrm{s,H_2}} + s_{\mathrm{H_2}}} x_{\mathrm{H_2}} \cdot I_{\mathrm{IN}}$
6	Death of sugars utilizers					-1			$\rho_{x_{\mathrm{su}}} = k_{\mathrm{d}} \cdot x_{\mathrm{su}}$
7	Death of amino acids utilizers						-1		$\rho_{x_{\mathrm{aa}}} = k_{\mathrm{d}} \cdot x_{\mathrm{aa}}$
8	Death of hydrogen utilizers							-1	$\rho_{\mathrm{H_2}} = k_{\mathrm{d}} \cdot x_{\mathrm{H_2}}$
									$I_{\mathrm{IN}} = \frac{s_{\mathrm{IN}}}{s_{\mathrm{IN}} + K_{\mathrm{s,IN}}}$

Table 4: Stoichiometry of reactions represented in the model.

Sugars (glucose) utilization	
$C_6H_{12}O_6 + 2H_2O \Rightarrow 2CH_3COOH + 2CO_2 + 4H_2$	(R_1)
$3C_6H_{12}O_6 \Rightarrow 2CH_3COOH + 4CH_3CH_2COOH + 2CO_2 + 2H_2O$	(R_2)
$C_6H_{12}O_6 \Rightarrow CH_3CH_2CH_2COOH + 2CO_2 + 2H_2$	(R_3)
$5C_6H_{12}O_6 + 6NH_3 \Rightarrow 6C_5H_7O_2N + 18H_2O$	(R_4)
Amino acid utilization	
$C_5H_{9.8}O_{2.7}N_{1.5} \Rightarrow (1 - Y_{aa}) \cdot \sigma_{ac,aa} CH_3COOH + (1 - Y_{aa}) \cdot \sigma_{pr,aa} CH_3CH_2COOH + Y_{IN,aa} NH_3 +$ $(1 - Y_{aa}) \cdot \sigma_{bu,aa} CH_3CH_2CH_2COOH + (1 - Y_{aa}) \cdot \sigma_{IC,aa} CO_2 + (1 - Y_{aa}) \cdot \sigma_{H_2,aa} H_2 + Y_{aa}\ C_5H_7O_2N$	(R_5^*)
Hydrogen utilization: methanogenesis reaction	
$4H_2 + CO_2 \Rightarrow CH_4 + 2H_2O$	(R_6)
$10H_2 + 5CO_2 + NH_3 \Rightarrow C_5H_7O_2N + 8H_2O$	(R_7)

*. The molecular formula of the average amino acid was calculated from the amino acid composition of alfalfa obtained from Feedipedia (`http://www.feedipedia.org/`). On the basis of the amino acid composition, a theoretical reaction was derived by following the procedure proposed by (Ramsay and Pullammanappallil, 2001). The overall reaction results from weighing the fermentation reactions of the individual amino acids by their molar fraction in the feed. For this overall reaction, the stoichiometric coefficients are $\sigma_{ac,aa} = 0.67, \sigma_{pr,aa} = 0.06, \sigma_{bu,aa} = 0.24, \sigma_{IC,aa} = 0.88, \sigma_{H_2,aa} = 0.84$. See Appendix A for further details on the derivation of the stoichiometry.

Table 5: Numerical values of the model parameters.

θ	Value	Reference
Constants and physicochemical and operational parameters		
K_{a,CO_2}	$5.13 * 10^{-7}$	(Batstone et al., 2002)
K_{a,NH_4}	$1.44 * 10^{-9}$	(Batstone et al., 2002)
$K_{a,VFA}$	$1.74 * 10^{-5}$	(Batstone et al., 2002)
K_{H,CO_2}	$2.46 * 10^{-2}$	(Batstone et al., 2002)
K_{H,CH_4}	$1.10 * 10-3$	(Batstone et al., 2002)
K_{H,H_2}	$7.23 * 10-4$	(Batstone et al., 2002)
K_w	$2.75 * 10^{-14}$	(Batstone et al., 2002)
P (bars)	1.01325	(Serment et al., 2016)
T (K)	312.15	(Serment et al., 2016)
V_l (L)	0.030	(Serment et al., 2016)
w_{aa} (g/mol)	134	http://www.feedipedia.org/ see Appendix A
w_{ac} (g/mol)	60.05	https://en.wikipedia.org/
w_{bu} (g/mol)	88.10	https://en.wikipedia.org/
w_{mb} (g/mol)	113	(Batstone et al., 2002)
w_{pr} (g/mol)	74.08	https://en.wikipedia.org/
w_{su} (g/mol)	180.16	https://en.wikipedia.org/

θ	L_iL_s	L_iH_s	H_iL_s	H_iH_s	Mean ± standard deviation	Reference
Estimated physicochemical parameters						
k_La (h^{-1})	1.01	1.01	1.11	1.13	1.07 ± 0.06	
s_{cat^+} (mol/L)	0.14	0.14	0.14	0.13	0.14 ± 0.0017	
Parameters associated with hydrolysis and cell lysis processes						
$f_{ch,x}$ (g/g)		0.20				(Reichl and Baldwin, 1975)
$f_{pro,x}$ (g/g)		0.55				(Reichl and Baldwin, 1975)
k_d (h^{-1})		$8.33 * 10-4$				(Batstone et al., 2002)
$k_{hyd,ndf}$ (h^{-1})		0.05				(Serment et al., 2011)
$k_{hyd,nsc}$ (h^{-1})	0.19	0.22	0.21	0.19	0.20 ± 0.015	
$k_{hyd,pro}$ (h^{-1})	0.20	0.19	0.25	0.25	0.22 ± 0.03	

Table 5: Numerical values of the model parameters.

θ	L_iL_s	L_iH_s	H_iL_s	H_iH_s	Mean ± standard deviation	Reference
Parameters associated with sugars utilization						
$K_{s,su}$ (mol/L)			$9.0 * 10{-}3$			(Baldwin et al., 1987)
$k_{m,su}$ (mol/(mol · h)	0.99	0.99	0.99	0.99	0.99 ± 9.0∗10−4	
$K_{s,IN}^{\star}$ (mol/L)			$2.0 * 10{-}4$			(Baldwin and Denham, 1979)
Y_{su} (mol/mol)	0.19	0.15	0.15	0.14	0.16 ± 0.02	
λ_1	0.46	0.44	0.41	0.40	0.43 ± 0.03	
λ_2	0.32	0.31	0.28	0.27	0.29 ± 0.02	
λ_3	0.22	0.25	0.31	0.32	0.28 ± 0.05	
Parameters associated with amino acids utilization						
$K_{s,aa}$ (mol/L)			$6.4 * 10{-}3$			(Baldwin et al., 1987)
$k_{m,aa}$ (mol/(mol · h)	3.53	2.36	1.0	1.0	1.98 ± 1.22	
Y_{aa} (mol/mol)	0.29	0.27	0.33	0.37	0.31 ± 0.05	
$\sigma_{ac,aa}$			0.67			See Appendix A
$\sigma_{bu,aa}$			0.24			See Appendix A
$\sigma_{pr,aa}$			0.062			See Appendix A
$\sigma_{H_2,aa}$			0.82			See Appendix A
$\sigma_{IC_2,aa}$			0.88			See Appendix A
Parameters associated with hydrogen utilization						
K_{s,H_2} (mol/L)			$5.84 * 10{-}6$			(Robinson and Tiedje, 1982)
k_{m,H_2} (mol/(mol · h)	13.33	15.40	13.62	13.37	13.93 ± 0.98	
Y_{H_2} (mol/mol)	0.0016	0.0016	0.0016	0.0016	0.0016 ± 0	

* This parameter is also associated with hydrogen utilization.

Table 6: Statistics for model evaluation

	NH_3 (mM)	Acetate (mM)	Butyrate (mM)	Propionate (mM)	CH_4 (μmol)	CO_2 (μmol)	H_2 (μmol)	pH
Slope	1.0	0.99	0.99	1.02	1.23	0.86	1.01	0.99
r^2	0.99	0.97	0.97	0.97	0.99	0.99	0.97	0.83
RMSE*	0.29	2.29	0.82	0.82	96.50	302.84	0.10	0.03
100 $\times$ CV(RMSE)$^\diamondsuit$	2.6	4.9	6.8	5.4	25.4	21.6	11.2	0.4
CCC *	0.99	0.98	0.98	0.98	0.93	0.96	0.98	0.91

$*$ Root mean squared error (RMSE).

$\diamondsuit$ Coefficient of variation of the RMSE (CV(RMSE)).

$\star$ Concordance correlation coefficient (CCC) proposed by Lin (1989)

Appendix A. Stoichiometry of amino acids fermentation

The second column of Table A.7 shows the average amino acid composition of dehydrated alfalfa obtained from Feedipedia (`http://www.feedipedia.org/`). The molecular formula for alfalfa was calculated from this information and the elementary composition of the individual amino acids. The resulting molecular formula was $C_{4.8}H_{9.4}O_{2.6}N_{1.2}$ which has 13.4% of nitrogen content. After correcting this value to 16% and rounding, we obtained the final molecular formula of the average amino acid $C_5H_{9.8}O_{2.7}N_{1.5}$. Table A.7 shows average stoichiometric coefficients for amino acid fermentation by anaerobic bacteria. These coefficients were extracted from the work of Ramsay and Pullammanappallil (2001) who selected dominant amino acid fermentation reactions from an inventory of reactions for different bacterial species.

The overall stoichiometry was obtained by multiplying the stoichiometric coefficients of each reaction by the molar fractions of the individual amino acids for alfalfa. It should be noted that other compounds such as minor VFA are also produced during amino acid fermentation, but they are not accounted for in the current overall reaction.

Table A.7: Overall stoichiometry for amino acid fermentation.

	Molar composition (%)	Acetate (mol/mol AA)	Propionate (mol/mol AA)	Butyrate (mol/mol AA)	CO_2 (mol/mol AA)	H_2 (mol/mol AA)
Arginine	4.0	0.5	0.5	0	1	-1
Histidine	1.5	1	0	0.5	1	0
Lysine	5.0	1	0	1	0	0
Tyrosine	2.8	1	0	0	1	1
Tryptophan	0.9	0	0	0	1	2
Phenylalanine	4.3	0	0	0	1	2
Cysteine	1.9	1	0	0	1	0.5
Methionine	1.3	0	1	0	1	1
Threonine	4.1	1	0	0.5	0	-1
Serine	6.2	1	0	0	1	1
Leucine/Isoleucine	13.5	0	0	0	1	2
Valine	8.3	0	0	0	1	2
Glutamine	10.2	1	0	1	1	0
Aspartate	11.9	1	0	0.5	2	2
Glycine	9.3	1	0	0	0	-1
Alanine	8.9	1	0	0	1	2
Proline	5.8	0.5	0.5	0	0	-1
Overall stoichiometry		0.67	0.06	0.24	0.88	0.84